

Kinetic modeling of the self-structure factor for gases

Lynn Groome*

Chemical Engineering, University of Florida, Gainesville, Florida 32611

James W. Dufty and Michael J. Lindenfeld†

Department of Physics, University of Florida, Gainesville, Florida 32611

(Received 5 July 1978)

A method for optimizing usual kinetic modeling techniques for determination of the dynamic structure factor from a given kinetic equation is investigated. The procedure has the potential to significantly reduce the calculational effort, thereby permitting future study of more complex kinetic equations currently being developed for dense gases. The exact low-density kinetic equation with step potential interaction including finite-collision-time effects is derived for calculation of the self-structure factor and used to illustrate and test the kinetic modeling.

I. INTRODUCTION

The classical dynamic-structure factor $S(k, \omega)$ is a directly measurable property of fluids in general (via neutron or light scattering) and provides one of the most detailed views of the dynamics of fluctuations in equilibrium fluids.¹ The measurement of $S(k, \omega)$ not only provides information about the properties of fluids, but also serves as a guidance for and test of theoretical models and approximation schemes for the statistical-mechanical description of fluids. In particular, an active subject of theoretical studies is the collision operator (or memory function) M that characterizes the linear kinetic equation governing the dynamics of the equilibrium fluctuations. For detailed comparison of theory and experiment two distinct problems may be identified. The first is an analysis of the many-body problem to determine an accurate approximate form of the collision operator appropriate for the fluid and state conditions being considered. A great deal of attention has been given to this problem in recent years² indicating the applicability of kinetic theory methods to liquids as well as gases. The second problem is a more technical and purely mathematical question of how to compute $S(k, \omega)$, once the kinetic equation has been determined, without substantial loss of accuracy. Clearly, an unambiguous test of a proposed kinetic theory by comparison with measured $S(k, \omega)$ requires that the errors induced by the second problem be small compared to the first. Presently, the most accurate studies of this kind³ are limited to simple gases (primarily hard spheres) and use a "kinetic-modeling" procedure that attempts to estimate the eigenfunctions of the collision operator and calculate as many eigenvalues (diagonal matrix elements) as possible to converge to an accurate determination of $S(k, \omega)$. These calculations typically require ~ 30 matrix elements of

the collision operator for errors estimated to be less than about 2%. Use of simple and tractable models with few matrix elements leads to qualitatively correct results, but large errors $\sim 10\%$. The objective here⁴ is to study the possibility of optimizing these kinetic models to obtain relatively good accuracy (a few percent), but maintaining the simplicity of needing only a few (well-chosen) matrix elements. No consideration will be given to the problem of determining the collision operator itself, except for a simple example to illustrate the procedure. Specifically, the exact low-density kinetic equation for the self-structure factor is derived using a step-potential interaction. Finite force range and collision time effects are discussed, along with the Boltzmann limit.

The scattering function is determined from the density-density correlation function $F(k, \omega)$ through

$$S(k, \omega) = 2\text{Re} F(k, \omega), \quad (1.1)$$

where $F(k, \omega)$ is given by

$$F(k, \omega) \equiv (1, h). \quad (1.2)$$

The scalar product of two functions of \vec{v} is defined by

$$(a, b) \equiv \int d\vec{v} \phi(v) a^*(\vec{v}) b(\vec{v}) \quad (1.3)$$

and $\phi(v)$ is the Maxwell-Boltzmann distribution. Also, in (1.2), $h(\vec{k}, \omega, \vec{v})$ is the solution to a formally exact kinetic equation (Fourier-Laplace transformed with respect to space and time) of the form⁵

$$(-i\omega + i\vec{k} \cdot \vec{v} - M)h = S(k) + nc(k)i\vec{k} \cdot \vec{v}(1, h). \quad (1.4)$$

Here $S(k)$ is the static structure factor, $c(k) = (S - 1)/S$ is the Fourier-transformed direct correlation function, n is the number density, and M is the k - ω -dependent collision operator. Equation (1.4) may be solved to give $S(k, \omega)$,

$$\frac{S(k, \omega)}{S(k)} = 2\text{Re} \frac{I(k, \omega)}{1 - nc(k)[1 + i\omega I(k, \omega)]} \quad (1.5)$$

with

$$I(k, \omega) \equiv (1, R1), \quad R \equiv (-i\omega + i\vec{k} \cdot \vec{v} - M)^{-1}. \quad (1.6)$$

For simple atomic fluids there are quite good theories for $S(k)$ and $c(k)$, and we shall consider such equilibrium properties as known.⁶ The essential dynamical properties of the fluid are contained in the collision operator M , occurring through the function $I(k, \omega)$ and further attention may be focused on calculation of the latter, assuming a given form for M . There are several approaches to such a calculation based mainly on constructing a solution to (1.4) by modeling the collision operator or constructing an appropriate variational principle. However, if attention is restricted only to the computation of $S(k, \omega)$ rather than attempting first an accurate construction of $h(\vec{k}, \omega, \vec{v})$ the problem may be somewhat simpler, although less general. Briefly, two categories of approximations may be identified.

a. Spectral decomposition of M . These models will be called BGK models (Bhatnagar, Gross, and Krook) or Gross-Jackson models.⁷ Essentially, the operator is assumed to have a resolution of the identity so that a spectral decomposition is possible, e.g.,

$$M = \sum_i \lambda_i \bar{P}_i, \quad (1.7)$$

where the \bar{P}_i are projection operators onto (possibly improper) eigenfunctions of M and λ_i are the corresponding eigenvalues. These eigenfunctions are not generally known so that a modified procedure is usually described, e.g.,

$$(f, Mg) = \sum_{\alpha} \sum_{\beta} (\psi_{\alpha}, M\psi_{\beta})(f, \psi_{\alpha})(\psi_{\beta}, g)$$

or, more compactly,

$$M = \sum_{\alpha} \sum_{\beta} M_{\alpha\beta} P_{\alpha} P_{\beta}, \quad (1.8)$$

$$M_{\alpha\beta} \equiv (\psi_{\alpha}, M\psi_{\beta}).$$

Here $\{\psi_{\alpha}\}$ represents an arbitrary complete set of functions and P_{α} are the associated projection operators. A kinetic model of order N then consists of approximating (1.8) by taking

$$M_{\alpha\beta} \equiv (\psi_{\alpha}, M\psi_{\beta}) \approx \lambda_N \delta_{\alpha\beta}, \quad \alpha, \beta \geq N \quad (1.9)$$

so that

$$M \approx \mathcal{O}M\mathcal{O} + \lambda_N(1 - \mathcal{O}) \equiv M_N. \quad (1.10)$$

Here $\mathcal{O} \equiv \sum_{\alpha=1}^{N-1} P_{\alpha}$. Thus M is taken to be exact in some $N - 1$ dimensional subspace and completely degenerate in the orthogonal complement to that subspace. With such a model, the correlation function may be determined from a system of N

coupled linear equations, once the $(\psi_{\alpha}, M\psi_{\beta})$ have been computed. As mentioned, typically $N \geq 30$ for present calculations. The probable reason for needing such large N lies in the complexity of the true spectrum of M , which may be expected to have a point spectrum near the origin with a continuum extending from some finite value to infinity. How accurately the latter is represented by the above for given N is not clear. More accuracy, and presumably convergence, is attained by increasing N .

b. Variational principle. There are standard methods for solving linear operator equations, approximately, by minimizing an appropriate functional. For determination of $I(k, \omega)$ such a functional is⁸

$$\mathcal{G}[f, g] \equiv (1, f) + (g, 1) - (g, R^{-1}f) \quad (1.11)$$

and where R is defined in Eq. (1.6). Consider the variation of \mathcal{G} through variation of f and g :

$$\delta\mathcal{G} = (1, \delta f) + (\delta g, 1) - (\delta g, R^{-1}f) - (g, R^{-1}\delta f).$$

Setting this variation equal to zero gives the requirements

$$0 = ([1 - R^{-1}g], \delta f) + (\delta g, [1 - R^{-1}f]). \quad (1.12)$$

Since the variations are arbitrary, this requires

$$f_e = R1, \quad g_e = R^*1 \quad (1.13)$$

at the extremum. (It is also possible to show that $g_e = f_e^*$.) Furthermore, the functional at extremum is equal to $I(k, \omega)$,

$$g_e(k, \omega) = I(k, \omega). \quad (1.14)$$

Thus a parametrized trial function f with $g = f^*$ may be adjusted to minimize $\mathcal{G}[f, g]$, to give the "best" solution to Eqs. (1.13) within the class of chosen trial functions, and hence a good estimate of $I(k, \omega)$. The weaknesses of the variational principle are the need for a good trial solution and lack of systematic way to improve the accuracy.

In the next section we reconsider the Gross-Jackson type of kinetic models with the objective of using low-order (small N) Gross-Jackson solutions as trial functions which are then optimized to give an accurate estimate of $S(k, \omega)$. The approach is somewhat similar in spirit to the variational principle just described although simpler in construction.

II. OPTIMIZATION OF KINETIC MODELS

The Gross-Jackson kinetic models, even for small N , are such that they reproduce the small ω, k limit (hydrodynamics or collisional range) and the large ω, k limits (free particles). A qualitative interpolation through the transition region is also provided. However the $N = 2$ Gross-Jack-

son model, for example, overestimates the non-Gaussian contribution to $S_s(k, \omega)$ by a factor of 4.⁹ The failure to get quantitatively accurate results in the transition region may be understood as follows. The resolvent operator R of Eq. (1.6) is essentially the inverse of the sum of a free streaming contribution $i\vec{k} \cdot \vec{v}$ and a collisional contribution M . The kinetic model treats $i\vec{k} \cdot \vec{v}$ exactly, but replaces M by its projection into a small subspace plus a degenerate approximation in the orthogonal subspace. In practice, the complete set of functions defining the kinetic modeling are orthogonal polynomials in \vec{v} , so that for small N the only information about M enters the model through low-order polynomial matrix elements of M ,

$$M_{\alpha\beta} \sim (v^\alpha, Mv^\beta); \quad n \leq \alpha, \quad m \leq \beta.$$

For vanishing $i\vec{k} \cdot \vec{v}$ the resolvent operator may be accurately determined from such low-order matrix elements (as is well known from the calculation of transport coefficients). However, in the transition region $i\vec{k} \cdot \vec{v}$ is of the same order of magnitude as the contribution of the collision operator and this additional velocity dependence of R effectively means that the domain of M is more severely tested. For example, near the free-particle limit R may be expanded as

$$R = R_0 + R_0 M R_0 + \dots, \quad R_0 \equiv (-i\omega + i\vec{k} \cdot \vec{v})^{-1} \quad (2.1)$$

or in terms of the function $I(k, \omega)$,

$$I(k, \omega) = (1, a) + (a^*, Ma) + \dots, \quad (2.2)$$

$$a \equiv R_0 1.$$

The second term in (2.2) is, in general, not at all well approximated by projection into a low-order polynomial subspace since the function a is not well approximated in such a manner. In summary, the problem of accurate kinetic-modeling centers substantially on the proper representation of the coupling in R between the $i\vec{k} \cdot \vec{v}$ and M contributions.

Nevertheless, the fact that the low-order Gross-Jackson kinetic models interpolate between the correct limits suggests that the general behavior of the function is essentially correct¹⁰ and simply needs to be properly parametrized. An obvious choice for parametrization is the degenerate eigenvalue in the order N kinetic model. Generally $\lambda_N \equiv (\psi_N, M\psi_N)$, but this choice itself is arbitrary. Instead, it may be possible to choose λ_N to optimize the kinetic model for calculating $S(k, \omega)$. To see how this might be done, consider the correlation function and write it as

$$\begin{aligned} I(k, \omega) &= (1, R1) \\ &= (1, R_N 1) + (1, R_N \Delta M R 1) \\ &= I_N(k, \omega) + (1, R_N \Delta M R 1). \end{aligned} \quad (2.3)$$

Here

$$\begin{aligned} \Delta M &\equiv M - M_N, \\ R &\equiv (-i\omega + i\vec{k} \cdot \vec{v} - M)^{-1} \\ R_N &\equiv (-i\omega + i\vec{k} \cdot \vec{v} - M_N)^{-1}, \end{aligned} \quad (2.4)$$

and M_N is the order N kinetic modeling operator, except with λ_N replaced by a free parameter $\lambda(k, \omega)$. The optimization consists of improving the kinetic model by choosing $\lambda(k, \omega)$ to "minimize" the second term in Eq. (2.3). In principle, $\lambda(k, \omega)$ may be chosen to make this term vanish,

$$(1, R_N \Delta M R 1) = 0, \quad (2.5)$$

leaving $I(k, \omega)$ given *exactly* by the kinetic model

$$I(k, \omega) = I_N(k, \omega). \quad (2.6)$$

This procedure departs considerably in spirit from the original kinetic modeling, since the condition determining $\lambda(k, \omega)$ is only guaranteeing an accurate value for $I(k, \omega)$, and not necessarily a good solution to the kinetic equation. Indeed, if a different correlation function were desired the corresponding condition similar to (2.5) would presumably give different values for $\lambda(k, \omega)$. Also, the practicality of this method rests on the assumption that reasonable and tractable approximations may be found for (2.5). The latter may be written more explicitly as

$$\lambda(k, \omega) = (1, R_N M_1 R 1) / (1, R_N [1 - \mathcal{P}] R 1), \quad (2.7)$$

where

$$M_1 \equiv M - \mathcal{P} M \mathcal{P}, \quad (2.8)$$

i.e., $\lambda(k, \omega)$ is given in terms of that part of M which acts in the subspace for which the kinetic model is not exact. The expression (2.7) is the basis for our optimization of low-order Gross-Jackson models, and several observations may be made. Equation (2.7) is only an implicit expression for λ (since R_N on the right side depends on λ) and it is not clear that unique or even reasonable solutions to this nonlinear integral equation exist. Furthermore, the presence of R in (2.7) means, as just noted, that a practical approximation scheme is required to obtain an explicit form for this integral equation. Finally, λ can no longer be associated in any simple or approximate way with a point in the spectrum of M , even if the ψ_α defining the kinetic model are eigenfunctions. It has been assumed that the order N of the kinetic model is chosen sufficiently large to give the proper qualitative behavior over the full range of k, ω values. In practice, this means the properties of M implied by the conservation laws must be retained to represent the transition to the hydrodynamic limit. For a simple fluid the kinetic model should be of order $N \geq 6$. For determination

of the self-structure factor (coherent neutron scattering) there is only one conservation law so that the kinetic model need only be of order $N \geq 2$. In both cases N is sufficiently small that an analytical determination of $I_N(k, \omega)$, and hence $S(k, \omega)$, is possible in terms of $\lambda(k, \omega)$.

Since the kinetic model is qualitatively correct it may be expected that $\lambda(k, \omega)$ should be a smooth function of k, ω , relative to $I(k, \omega)$. Therefore, a simple and reasonable approximation scheme for the evaluation of λ from Eq. (2.7) is to expand R about the kinetic model resolvent operator

$$R = R_N + R_N \Delta M R_N + \dots \quad (2.9)$$

Retaining only the leading term gives as a first approximation for λ the equation

$$\lambda(k, \omega) = (1, R_N M_1 R_N) / (1, R_N [1 - \mathcal{P}] R_N) + \dots \quad (2.10)$$

The expansion (2.10) is not simply an expansion of λ in powers of ΔM since the resolvent operators R_N on the right-hand side of (2.10) also are functionals of ΔM through their dependence on λ . Actually the expansion results from considering λ as a functional of ΔM and λ itself [Eq. (2.7)], and expanding in powers of ΔM holding λ constant. Truncation of the expansion (2.10) corresponds to a "renormalization" of the corresponding expansion for I . To see this, consider the expansion of I in powers of ΔM holding λ constant,

$$I = (1, R_N) + (1, R_N \Delta M R_N) + \dots \quad (2.11)$$

The convergence of this perturbation expansion may be improved by requiring the second term on the right-hand side of (2.11) to vanish (i.e., the

$$\lambda_{\text{var}}(k, \omega) = \frac{1}{2} \left(\frac{(1, R_N M_1 R_N [1 - \mathcal{P}] R_N) + (1, R_N [1 - \mathcal{P}] R_N M_1 R_N)}{(1, R_N [1 - \mathcal{P}] R_N [1 - \mathcal{P}] R_N)} \right). \quad (2.15)$$

According to the variational principle, this result for λ is now to be used in (2.14) to give an estimate for $I(k, \omega)$:

$$I_{\text{var}}(k, \omega) = (1, R_N) + (1, R_N \Delta M R_N). \quad (2.16)$$

This result differs from the above optimization scheme in two important respects. First the variational expression for λ , Eq. (2.15) is similar to, but somewhat more complicated than that of Eq. (2.13). Additionally, the variational estimate of I is not simply given by the Gross-Jackson form for I , but requires also evaluation of the second term on the right-hand side of (2.16). Indeed the difference between the variational method and the above described optimization scheme is that the latter requires that λ be determined from the condition that the second term on the right-hand side of Eq.

first correction to the order- N kinetic model),

$$(1, R_N \Delta M R_N) = 0 \quad (2.12)$$

or

$$\lambda = (1, R_N M_1 R_N) / (1, R_N [1 - \mathcal{P}] R_N), \quad (2.13)$$

which is just the leading term in the expansion of λ , Eq. (2.10). In practice, it does not appear useful to attempt calculation beyond the form given by the leading term. It should be noted that even with truncation at the leading term, the expression (2.13) may still be made arbitrarily accurate by increasing the order of the kinetic model, N . In summary, our proposed optimization of the order- N Gross-Jackson kinetic model for determination of $S(k, \omega)$ consists of equations (1.5) and (2.6), with $\lambda(k, \omega)$ determined approximately from (2.13).

Before studying the determination of $\lambda(k, \omega)$ from Eq. (2.13), it is interesting to see the form of λ that would result from application of the variational principle. Assuming for the trial function f , the solution to the order- N kinetic model, the functional (1.11), becomes

$$\begin{aligned} \mathcal{J}[f, g] &= 2(1, R_N) - (1, R_N R^{-1} R_N) \\ &= (1, R_N) + (1, R_N \Delta M R_N). \end{aligned} \quad (2.14)$$

Minimization of the functional by variation of λ requires λ satisfy

$$\begin{aligned} \frac{\partial I}{\partial \lambda} = 0 &= (1, R_N [1 - \mathcal{P}] R_N \Delta M R_N) \\ &+ (1, R_N \Delta M R_N [1 - \mathcal{P}] R_N) \end{aligned}$$

or

(2.16) vanish, while the variational method determines a value for this term such as to yield an extremum. There is no obvious way to determine which of these two estimates of I is more accurate (a determination which may in fact change with k, ω). However, we choose not to pursue the variational method due to the significantly greater calculational effort required.

To study the utility and accuracy of the optimization scheme defined by equations (1.5), (2.6), and (2.13), the remainder of our investigations here will be limited to the somewhat simpler problem of calculating the self-structure factor $S_s(k, \omega)$, determined from a kinetic equation like (1.4) with $S(k) = 1$, $c(k) = 0$, and a different collision operator denoted M_s ,

$$S_s(k, \omega) = 2\text{Re} I_s(k, \omega), \quad (2.17)$$

$$I_s(k, \omega) = (1, R_s 1), \quad (2.18)$$

$$R_s(k, \omega) = (-i\omega + i\vec{k} \cdot \vec{v} - M_s)^{-1}. \quad (2.19)$$

The above optimization scheme now applies to I_s with only the replacement everywhere of M by M_s . To be more explicit, a specific choice of N should be made to define the Gross-Jackson model to be optimized. Since the objective here is to reduce the calculational effort the smallest value of N will be chosen, consistent with the above mentioned requirement that the conservation laws be accurately retained. For self-correlations there is only one conservation law, conservation of mass, reflected by the property

$$(1, M_s h) = (h, M_s 1) = 0 \quad (2.20)$$

for arbitrary h (i.e., the function 1 is an eigenfunction of M_s and its adjoint with zero eigenvalue). The lowest-order kinetic model incorporating (2.20) is $N=2$,

$$M_s \sim 0P + \lambda(1 - P), \quad (2.21)$$

where P is the projection operator onto 1,

$$Ph = 1(1, h). \quad (2.22)$$

The optimized Gross-Jackson estimate of $S_s(k, \omega)$ is then defined by

$$S_s(k, \omega) = 2\text{Re}(1, R_2 1), \quad (2.23)$$

$$R_2 \equiv (-i\omega - \lambda + i\vec{k} \cdot \vec{v} + \lambda P)^{-1}, \quad (2.24)$$

with λ determined from

$$\lambda(k, \omega) = \frac{(1, R_2 M_s R_2 1)}{(1, R_2 [1 - P] R_2 1)}. \quad (2.25)$$

The effect of the projection operator may be evaluated using the identity

$$R_2 = G - G\lambda P R_2 \quad (2.26)$$

with

$$G(k, \omega) \equiv (-i\omega - \lambda + i\vec{k} \cdot \vec{v})^{-1} \quad (2.27)$$

to give

$$S_s(k, \omega) = 2\text{Re} \frac{(1, G)}{1 + \lambda(1, G)}, \quad (2.28)$$

$$\lambda(k, \omega) = \frac{(G^*, M_s G)}{(G^*, G) - (1, G)^2}. \quad (2.29)$$

It is convenient to introduce a dimensionless form of $S_s(k, \omega)$,

$$\mathfrak{R} \equiv kv_0 S_s(k, \omega),$$

where v_0 is the thermal velocity, $v_0 = (2/\beta m)^{1/2}$, $\beta \equiv (k_B T)^{-1}$. Then equations (2.28) and (2.29) may be written in the form

$$\mathfrak{R}(x, y) = 2\text{Re} \left(\frac{\phi(z)}{i + \lambda^* y \phi(z)} \right), \quad (2.30)$$

$$\lambda^*(z) = \frac{k^2 v_0^2}{2\lambda_0} \frac{(G^*, M_s G)}{[1 + z \phi(z) + \frac{1}{2} \phi^2(z)]}, \quad (2.31)$$

where $\phi(z)$ is the complex plasma dispersion function,

$$\phi(z) \equiv \frac{1}{\sqrt{\pi}} \int_{-\infty}^{\infty} dp \frac{e^{-p^2}}{p - z} \quad (2.32)$$

and the variables x , y , z , and λ^* are defined by

$$z \equiv x - i\lambda^* y, \quad x \equiv \omega/kv_0, \quad y \equiv \lambda_0/kv_0, \quad \lambda^* \equiv \lambda/\lambda_0. \quad (2.33)$$

Finally, λ_0 is a constant frequency to be chosen for convenience, typically of the order of the collision frequency. The variable x is chosen because in the free-particle limit \mathfrak{R} depends on ω and k only through x ,

$$\mathfrak{R}(x, y) \Big|_{\lambda=0} = 2\text{Im} \phi(z) \Big|_{\lambda=0} = 2\sqrt{\pi} e^{-x^2}. \quad (2.34)$$

Also, y may be interpreted as a measure of the relative importance of collisions (through λ_0) and free streaming (through kv_0). Hence $y \rightarrow 0$ corresponds to the free-particle limit while $y \rightarrow \infty$ corresponds to the collisional or hydrodynamic limit. To suggest a natural choice for λ_0 we first consider the hydrodynamic limit of λ ,

$$\lim_{y \rightarrow \infty} \lambda(x, y) = \frac{2}{v_0^2} (\hat{k} \cdot \vec{v}, M_s \hat{k} \cdot \vec{v}), \quad (2.35)$$

where \hat{k} is a unit vector in the direction of \vec{k} , and the corresponding limit on the y dependence (if any) of M_s is also implied. The right-hand side of (2.35) is just the usual value λ_2 assigned to the Gross-Jackson model when Sonine or Hermite polynomials are used as the complete set of functions, the first two of which are chosen to be

$$\psi_1(\vec{v}) = 1, \quad \psi_2(\vec{v}) = (\sqrt{2}/v_0) \hat{k} \cdot \vec{v}$$

so that (2.35) is recognized as

$$\lim_{y \rightarrow \infty} \lambda(x, y) = (\psi_2, M_s \psi_2) = \lambda_2. \quad (2.36)$$

The optimized model and the usual Gross-Jackson model therefore agree in the hydrodynamic limit. It may be noted that in kinetic modeling there is the freedom to choose an ordering among the complete set of functions. Thus when the $N-1$ subspace is chosen, the specific function ψ_N defining λ_N must be one of the remaining members of the complete set, but is otherwise arbitrary. Usually, the ordering is selected according to the magnitude of the diagonal matrix element $M_{\alpha\alpha}$, or the order of the polynomial defining ψ_N ; here, however, the limit value of λ is determined automatically. Since this value is also a measure of the collision operator in the collisional (hydrodynamic) limit, it is a natural value to choose for λ_0 to define the dimensionless quantity λ^* ,

$$\lambda_0 \equiv \left| \lim_{y \rightarrow \infty} \lambda(x, y) \right|. \quad (2.37)$$

It is further possible to recognize that the first Enskog approximation to the self-diffusion coefficient is then

$$D = (\beta m \lambda_0)^{-1} \quad (2.38)$$

so that, for example, the variable y becomes

$$y = v_0 / 2Dk. \quad (2.39)$$

It has been suggested that a variety of gases interacting via different intermolecular potentials is well described by a universal expression for $\mathcal{R}(x, y)$ when the choice (2.39) is made.⁹ Further comment on this point will be made in Sec. IV.

To summarize, the self-scattering function is described by Eq. (2.30). The usual $N=2$ Gross-Jackson model (in this case, single relaxation time model) corresponds to $\lambda^* = -1$. However, the definition of λ^* , given by (2.31), is in terms of a matrix element of M_s with respect to the function $G(k, \omega)$ whose form varies with k and ω and hence samples different portions of the spectrum of M_s for different values of these variables. For small k and ω , G behaves as a polynomial in \vec{v} but for large k and ω , G behaves more like the free-particle solution to the kinetic equation. This optimization scheme is essentially the same as that suggested by Hess¹¹ for calculation of pressure-broadened atomic line shapes. In the latter case the "collision operator" describes collision-induced transitions between internal atomic states and the correlation function of interest is the atomic-dipole autocorrelation function. Although no calculations appear to have been done for this case, the results given here suggest that the method would be useful for study of the correlation between Doppler and pressure broadening.¹²

III. TESTS OF THE OPTIMIZATION SCHEME

In this section the self-structure factor is calculated from two idealized kinetic equations for which accurate results for $S_s(k, \omega)$ are available. In this way the $N=2$ Gross-Jackson kinetic model and its optimization may be compared and the extent of improvement on optimization assessed. The first case is the Fokker-Planck equation, for which $S_s(k, \omega)$ may be calculated exactly. The second example is the hard-sphere Boltzmann-Lorentz-Enskog equation, for which $S_s(k, \omega)$ is known from an $N=35$ kinetic model.

A. Fokker-Planck equation

The collision operator M_s for a fluid described by a Fokker-Planck equation¹³ is given by

$$\begin{aligned} M_s &\rightarrow M_{\text{FP}}, \\ M_{\text{FP}} &\equiv \gamma \left(\frac{1}{2} v_0^2 \nabla_v^2 - \vec{v} \cdot \vec{\nabla}_v \right), \end{aligned} \quad (3.1)$$

where γ is the friction constant. The exact self-structure factor may be calculated directly from the known Green's function for the Fokker-Planck equation,

$$S_s(k, \omega) = 2\text{Re} \int_0^\infty dt e^{-i\omega t} \exp\left(\frac{-k^2}{\beta m \gamma} t + \frac{k^2}{\beta m \gamma^2} (1 - e^{-\gamma t})\right)$$

or

$$\mathcal{R}(x, y) = 2 \int_0^\infty dt \cos(xt) \exp\left(\frac{-t}{2y} + \frac{1}{2y^2} (1 - e^{-yt})\right). \quad (3.2)$$

Now consider the calculation of $\mathcal{R}(x, y)$ for the Fokker-Planck equation from the optimized $N=2$ Gross-Jackson kinetic model, (2.30) and (2.31),

$$\mathcal{R}(x, y) = 2\text{Re}\{\phi(z)/[i + \lambda^* \phi(z)]\}, \quad (3.3)$$

$$\lambda^* = \frac{(kv_0)^2}{2\gamma} \frac{(G^*, M_{\text{FP}}G)}{[1 + z\phi(z) + \frac{1}{2}\phi^2(z)]}, \quad (3.4)$$

where use has been made of the fact that λ_0 , as defined by (2.37) and (2.35), is equal to the friction constant γ . Substitution of (3.1) into (3.4) gives

$$\lambda^* = \frac{(kv_0)^4}{4} \frac{(1, G^4)}{[1 + z\phi(z) + \frac{1}{2}\phi^2(z)]}. \quad (3.5)$$

The use of the identity

$$\begin{aligned} (1, G^n) &= [2/(n-1)(kv_0)^2] \\ &\times [(1, G^{n-2}) + (-i\omega + \lambda)(1, G^{n-1})] \end{aligned}$$

gives finally the equation for λ^* ,

$$\lambda^* = \frac{1}{3} \frac{[1 - z^2 + z(\frac{3}{2} - z^2)\phi(z)]}{[1 + z\phi(z) + \frac{1}{2}\phi^2(z)]}. \quad (3.6)$$

Since the right-hand side is a highly nonlinear functional of λ^* there is no assurance of a unique solution for given x and y . However, uniqueness is fixed by the condition that the real and imaginary parts be continuously generated from the value $\lim_{y \rightarrow \infty} \lambda^*(x, y) = -1$. Solution to (3.6) is obtained for each value of the pair x, y by iteration, typically with convergence to within 1% after four iterations. As noted, both the usual and optimized Gross-Jackson kinetic models agree in the free-particle (small y) and hydrodynamic (large y) limits. The best test of kinetic modeling is, therefore, in the transition region corresponding here to roughly $0.3 < y < 3$. Figure 1 shows a comparison of the $N=2$ Gross-Jackson kinetic model ($\lambda^* = -1$) calculation of $\mathcal{R}(x, y)$ at $y = 1.25$ with the corresponding optimized and exact results. The maximum error of the Gross-Jackson model is about 12% at $x=0$ whereas the optimized model has a maximum error of 2% at $x=0$. Figure 2 shows that this improvement is uniformly good for all y with comparison of the calculated halfwidth

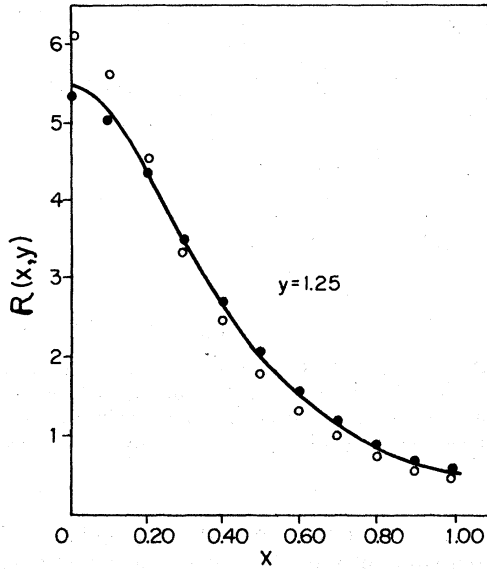


FIG. 1. Self-structure factor $R(x, y)$ for the Fokker-Planck model; exact solution (—), $N=2$ Gross-Jackson model (O), and optimized $N=2$ model (●).

of $R(x, y)$ at half maximum as a function of y . Again the optimized calculation is a considerable improvement over the usual $N=2$ kinetic model results.

B. Hard-sphere Boltzmann-Lorentz-Enskog equation

The Fokker-Planck collision operator has only a point spectrum at equally spaced intervals and simple eigenfunctions (Hermite polynomials). Generally, the collision operator for a fluid may be expected to be considerably more complex,^{13,14} with both discrete and continuous spectra, and therefore more difficult to model. A more realistic test of the kinetic modeling than the Fokker-Planck equation is provided by the hard-sphere Boltzmann-Enskog equation¹⁵ (Boltzmann-Lorentz-Enskog equation, for self-correlations). Although this is a rather idealized potential model, it adequately represents many properties of simple

$$(G^*, M_E G) = n\sigma^2 g(\sigma) \int d\vec{v} d\vec{v}_2 \phi(v) \phi(v_2) \int d\Omega \hat{r} \cdot \vec{g} \theta(-\hat{r} \cdot \vec{g}) (-i\omega + i\vec{k} \cdot \vec{v} - \lambda)^{-1} \\ \times [(-i\omega + i\vec{k} \cdot \vec{v} - \lambda)^{-1} - (-i\omega + i\vec{k} \cdot \vec{v}' - \lambda)^{-1}], \quad (3.10)$$

and for hard spheres Eq. (2.37) gives $\lambda_0 = \frac{4}{3}\sqrt{2\pi} n\sigma^2 g(\sigma) v_0$. This eight-dimensional integral may be reduced to a two-dimensional integral; the details are provided for the step-potential model in Appendix B and will not be repeated here. The calculational form of λ^* is found to be

$$\lambda_{hs}^* = \frac{A_{hs}(z)}{[1 + z\phi(z) + \frac{1}{2}\phi^2(z)]} \quad (3.11)$$

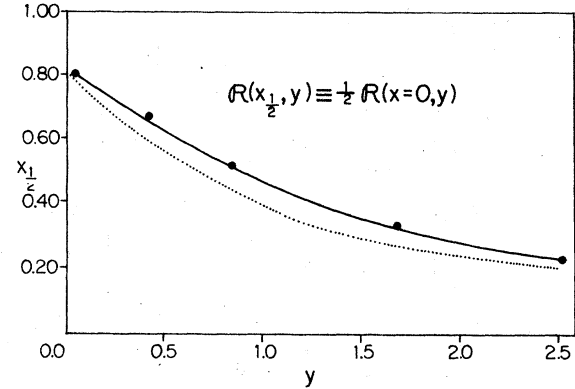


FIG. 2. Halfwidth at half maximum ($x_{1/2}$) for the Fokker-Planck model; exact solution (—), $N=2$ Gross-Jackson model (---), and optimized $N=2$ model (●).

dense atomic fluids when a suitable choice of hard-sphere diameter is made, and the collision operator reflects most of the mathematical structure of the operators for more general force laws. The Boltzmann-Lorentz-Enskog collision operator results from retaining binary collision contributions modified by a class of excluded volume effects induced by the presence of particles other than the colliding pair. The form of the collision operator is given by

$$M_E \rightarrow M_E, \quad (3.7)$$

$$M_E[h] = n\sigma^2 g(\sigma) \int d\vec{v}_2 \phi(v_2) \int d\Omega \hat{r} \cdot \vec{g} \theta(-\hat{r} \cdot \vec{g}) \\ \times [h(\vec{v}) - h(\vec{v}')]. \quad (3.8)$$

Here $\vec{g} \equiv \vec{v}_2 - \vec{v}$ is the relative velocity, $g(\sigma)$ is the hard-sphere radial distribution function at hard-sphere diameter σ and \vec{v}' is the scattered velocity (see Appendix A for more explicit definition of the notation). Substitution of Eq. (3.7) into Eq. (2.31) for λ^* gives

$$\lambda^* = \frac{(kv_0)^2}{2\lambda_0} \frac{(G^*, M_E G)}{[1 + z\phi(z) + \frac{1}{2}\phi^2(z)]} \quad (3.9)$$

with

$$A_{hs}(z) = \frac{3}{\sqrt{\pi}} \int_{-\infty}^{\infty} du e^{-u^2} \\ \times \int_0^{\infty} ds s e^{-s^2} \left[\frac{s^2}{(u + \sqrt{2}z)^2 - s^2} - \frac{1}{4} \ln^2 \left(\frac{u + \sqrt{2}z + s}{u + \sqrt{2}z - s} \right) \right]. \quad (3.12)$$

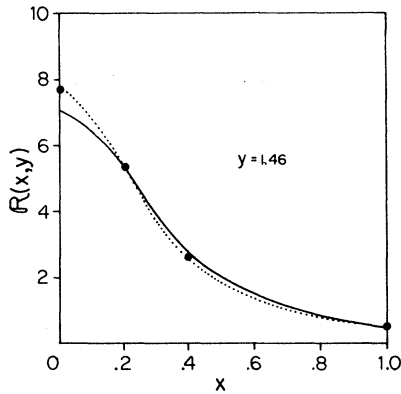


FIG. 3. $R(x,y)$ for Boltzmann-Lorentz-Enskog hard-sphere kinetic equation; $N=2$ Gross-Jackson model (—), optimized $N=2$ model (---), and $N=35$ Gross Jackson model (●).

The function $A_{hs}(z)$ is readily evaluated by numerical integration (see Appendix B) and an iterative solution to (3.11) is again found to converge to within 1% after four iterations. Figure 3 shows a comparison of $N=2$ Gross-Jackson and optimized kinetic models with a presumed convergent $N=35$ kinetic model, for $y=1.46$. The corresponding percent errors of the $N=2$, $N=7$, and optimized $N=2$ models, relative to the $N=35$ model, are shown in Fig. 4; the halfwidths at half maximum are shown in Fig. 5. These results indicate that the optimized $N=2$ model is a significant improvement over the entire range of y values. Further-

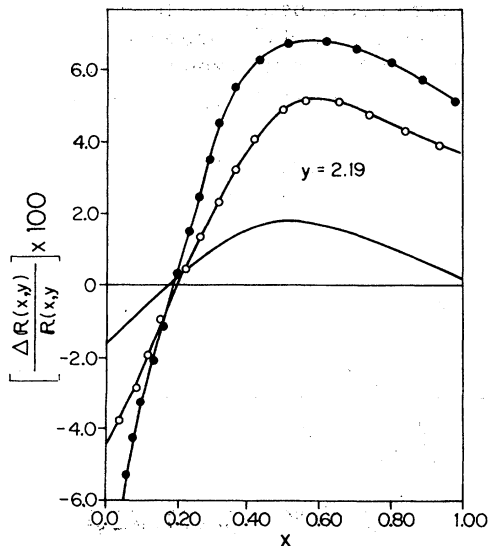


FIG. 4. Percent deviation from $N=35$ model for Boltzmann-Lorentz-Enskog hard-sphere results; $N=2$ Gross-Jackson model (●), $N=7$ Gross-Jackson model (○), and optimized $N=2$ model (—).

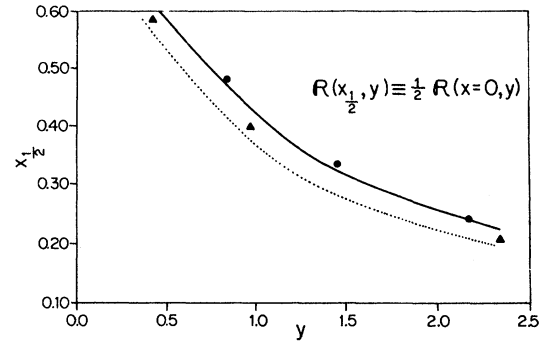


FIG. 5. Halfwidth at half maximum for Boltzmann-Lorentz-Enskog hard-sphere results; $N=35$ Gross-Jackson model (—), $N=7$ Gross-Jackson model (▲), $N=2$ Gross-Jackson model (---), and optimized $N=2$ model (●).

more, computer time for calculation of $R(x,y)$ at a given value of y is of the order of 1 min compared with several hours¹⁶ for calculation of all the matrix elements in the $N=35$ kinetic model.

Since the improvement over the usual $N=2$ model is entirely controlled by λ^* the differences are better illustrated by plotting the real and imaginary parts of this parameter. Figure 6 shows that λ^* decreases from -1 as the transition is made from the hydrodynamic to free-particle limits. Also, for large x , λ^* approaches -1 for all y , so that variation of λ^* with x is greatest in the free-particle region. Similarly, the imaginary part of λ^* is zero for all x at sufficiently large y , but increases with x as y decreases. As anticipated, the variation of λ^* with x and y is smooth, confirming the supposition that λ^* should be an easier function to approximate than R itself.

IV. DILUTE GAS-STEP POTENTIAL

The Boltzmann-Lorentz-Enskog collision operator just considered is independent of k, ω . Furthermore, the temperature dependence of the matrix

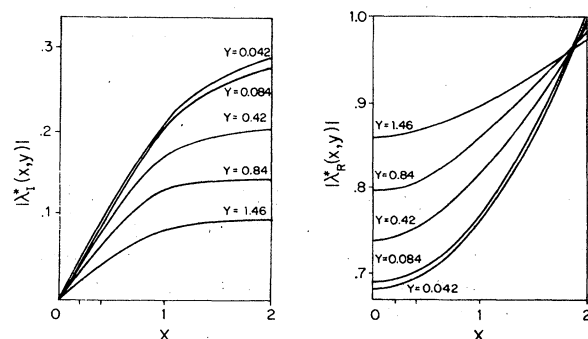


FIG. 6. Real and imaginary parts of λ^* for the Boltzmann-Lorentz-Enskog kinetic model (optimized $N=2$ case), for different values of y .

elements of this operator may be simply removed by proper normalization. Generally, the collision operator for more realistic potentials, or more accurate treatment of density effects, depends non-trivially on all of these parameters.^{5,17} To illustrate this dependence and to show that the optimization scheme remains tractable for other potential models, the exact low-density collision operator for a fluid interacting via a step-potential interaction is discussed in this section.¹⁸ The step potential is defined by

$$V(r_{ij}) = \begin{cases} 0 & \text{for } r_{ij} \geq \sigma \\ V_0 & \text{for } r_{ij} < \sigma, \end{cases} \quad (4.1)$$

where r_{ij} denotes the relative coordinate of the pair of particles ij and V_0 is a constant. The de-

$$\begin{aligned} \Delta M[h] = n\sigma^2 \int d\vec{v}_2 \phi(v_2) \int d\Omega (\hat{r} \cdot \vec{g}) [\theta(-\hat{r} \cdot \vec{g}) \theta((\hat{r} \cdot \vec{g})^2 - 4V_0/m) \\ \times \{1 - \exp[i(\omega - \vec{k} \cdot \vec{v})T'']\} [h(\vec{v}'') - h(\vec{v}')] \\ - \theta(\hat{r} \cdot \vec{g}) e^{-\beta V_0} \{1 - \exp[i(\omega - \vec{k} \cdot \vec{v})T]\} [h(\vec{v}) - h(\vec{v}^*)]] . \end{aligned} \quad (4.5)$$

The velocities \vec{v}' , \vec{v}'' , \vec{v}''' , and \vec{v}^* correspond to the four types of possible complete and partial collisions¹⁹: (i) \vec{v}' is the scattered velocity for specular collisions at the well edge [Fig. 7(a)]. (ii) \vec{v}'' is the scattered velocity for partial penetrating collisions [Fig. 7(b)]. (iii) \vec{v}''' is the scattered velocity for completed penetrating collisions [Fig. 7(b)]. (iv) \vec{v}^* is the scattered velocity for partial separating collisions [Fig. 7(e)]. The contribution of collisions in Fig. 7(c) have been incorporated into those of Fig. 7(e). The remaining notation is defined in Appendix A. The collision operator (4.3) is the exact low-density form for all k and ω . The dependence on k and ω is due to the finite value of collision times T and T'' associated with the partial collisions defining v^* and v'' . When these times are small relative to the corresponding times of the physical phenomena being studied (e.g., $\omega T \ll 1$, $kv_0 T \ll 1$, etc.) the usual k -, ω -independent Boltzmann form (4.4) results. This and other limits follow directly from Eqs. (4.3)–(4.5).

Boltzmann limit: ($k\sigma \ll 1$, $\omega/\lambda_0 \ll 1$)

In this case the factors f and f'' , defined in Eq. (A21), go to zero when space and time scales are measured in units of σ and λ_0^{-1} , respectively. Therefore, $\Delta M \rightarrow 0$ and

$$\lim_{\substack{k\sigma \ll 1 \\ \omega/\lambda_0 \ll 1}} M_{sp} = M_B,$$

where M_B is defined by Eq. (4.4).

ivation of the collision operator is given in Appendix A, with the result,

$$M_S \rightarrow M_{sp}, \quad (4.2)$$

$$M_{sp} = M_B + \Delta M, \quad (4.3)$$

where M_B is the Boltzmann-Lorentz operator for the step potential,

$$\begin{aligned} M_B[h] = n\sigma^2 \int d\Omega d\vec{v}_2 \phi(v_2) \hat{r} \cdot \vec{g} \theta(-\hat{r} \cdot \vec{g}) \\ \times \{ \theta(4V_0/m - (\hat{r} \cdot \vec{g})^2) [h(\vec{v}) - h(\vec{v}')] \\ + \theta((\hat{r} \cdot \vec{g})^2 - 4V_0/m) [h(\vec{v}) - h(\vec{v}'')] \} \end{aligned} \quad (4.4)$$

and ΔM represents the dependence of k and ω ,

Hard-sphere limit: ($\beta V_0 \rightarrow \infty$)

$$\begin{aligned} \lim_{\beta V_0 \rightarrow \infty} M_{sp}[h] = n\sigma^2 \int d\Omega \int d\vec{v}_2 \phi(v_2) \hat{r} \cdot \vec{g} \theta(-\hat{r} \cdot \vec{g}) \\ \times [h(\vec{v}) - h(\vec{v}''')] = M_{hs}[h]. \end{aligned} \quad (4.6)$$

The hard-sphere result M_{hs} agrees with M_B , Eq. (3.8), in the low-density limit.

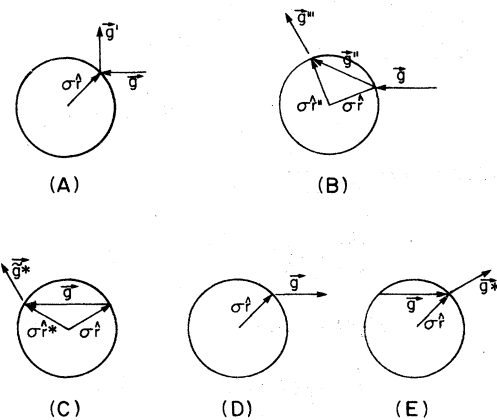


FIG. 7. Collision dynamics for the repulsive step potential at the potential radius: (a) the case $r = \sigma^+$, $\hat{r} \cdot \vec{g} < 0$, $(\hat{r} \cdot \vec{g})^2 < 4V_0/m$; (b) the case $r = \sigma^+$, $\hat{r} \cdot \vec{g} < 0$, $(\hat{r} \cdot \vec{g})^2 > 4V_0/m$; (c) the case $r = \sigma^+$, $\hat{r} \cdot \vec{g} > 0$; (d) the case $r = \sigma^-$, $\hat{r} \cdot \vec{g} < 0$; (e) $r = \sigma^-$, $\hat{r} \cdot \vec{g} > 0$.

High-frequency (short time) limit: ($\omega T \rightarrow \infty$)

In this limit f and f'' go to 1 [in the sense that integration with respect to a smooth function of (\vec{v}, θ) vanishes in this limit]. Therefore,

$$\begin{aligned} \lim_{\omega T \rightarrow \infty} M_{sp}[h(\vec{v})] = & n\sigma^2 \int d\vec{v}_2 \phi(v_2) \int d\Omega \hat{r} \cdot \vec{g} [\theta(-\hat{r} \cdot \vec{g}) \{ \theta(4V_0/m - (\hat{r} \cdot \vec{g})^2) [h(\vec{v}) - h(\vec{v}')] \\ & + \theta((\hat{r} \cdot \vec{g})^2 - 4V_0/m) [h(\vec{v}) - h(\vec{v}'')] \} \\ & - \theta(\hat{r} \cdot \vec{g}) e^{-\beta V_0} [h(\vec{v}) - h(\vec{v}^*)]] . \end{aligned} \quad (4.7)$$

This operator represents the three types of collisions that can occur instantaneously.

Thus all expected limits are verified.

A. Boltzmann limit

Consider first the effects of the βV_0 dependence in M_{sp} without regard to the k and ω dependence, i.e., in the Boltzmann limit. It will be shown below that for dilute gases the Boltzmann limit is indeed accurate for calculation of $\mathcal{R}(x, y)$. Since

βV_0 is a measure of the interaction energy relative to thermal energy it is expected that collisional narrowing of $\mathcal{R}(x, y)$ should increase with increasing βV_0 , for given k . Substitution of (4.4) into (2.31) gives the equation determining λ^* for this case,

$$\lambda_{sp}^*(x, y) = \frac{(kv_0)^2}{2\lambda_0} \frac{(G^*, M_B G)}{[1 + z\phi(z) + \frac{1}{2}\phi^2(z)]} \quad (4.8)$$

with

$$\begin{aligned} (G^*, M_B G) = & n\sigma^2 \int d\vec{v} \phi(v) \int d\vec{v}_2 \phi(v_2) \int d\Omega (\hat{r} \cdot \vec{g}) \theta(-\hat{r} \cdot \vec{g}) \\ & \times G(\vec{k}, \omega, \vec{v}) \{ \theta(4V_0/m - (\hat{r} \cdot \vec{g})^2) [G(\vec{k}, \omega, \vec{v}) - G(\vec{k}, \omega, \vec{v}')] \\ & + \theta((\hat{r} \cdot \vec{g})^2 - 4V_0/m) [G(\vec{k}, \omega, \vec{v}) - G(\vec{k}, \omega, \vec{v}'')] \} . \end{aligned} \quad (4.9)$$

The eight-dimensional integrals in Eq. (4.9) may be reduced to nested three-dimensional integrals. The details are given in Appendix B with the resulting expression for λ^* ,

$$\lambda_{sp}^*(x, y) = \frac{A_{sp}(z, \beta V_0)}{[1 + z\phi(z) + \frac{1}{2}\phi^2(z)]} , \quad (4.10)$$

$$A_{sp}(z, \beta V_0) = \frac{3}{\sqrt{\pi}} \int_{-\infty}^{\infty} du e^{-u^2} \int_0^{\infty} ds s e^{-s^2} \times B(u, s, \beta V_0, z) ,$$

$$B(u, s, \beta V_0, z) = \frac{s^2}{(u + \sqrt{2}z)^2 - s^2} - \sum_{i=0}^{\infty} Q_i^2 \left(\frac{u - \sqrt{2}z}{s} \right) C_i(s, \beta V_0) .$$

$$\begin{aligned} C_{i \neq 0}(s, \beta V_0) = & a^2(2l+1)\theta(s^2 - \beta V_0) \\ & \times \int_0^1 dq \{ P_i [2[aq + (1 - a^2q)^{1/2} \\ & \times (1 - q)^{1/2}]^2 - 1] \\ & - P_i(2a^2q - 1) \} , \end{aligned} \quad (4.11)$$

$$C_0(s, \beta V_0) = 1 .$$

Here Q_i are the Legendre functions of the second

kind for complex argument and P_i are the Legendre polynomials. Also $a^2 \equiv (1 - \beta V_0/s^2)$. The $l=0$ term reproduces the hard-sphere result, Eq. (3.12) (aside from the Enskog factor g). The calculational effort to determine λ_{sp}^* from (4.10) is not significantly greater than that for the hard-sphere case, and the computer time to calculate $\mathcal{R}(x, y)$ for given y is still of the order of minutes. Typically 3 to 10 terms in the l sum are required. Figure 8 shows \mathcal{R} in the transition region for $\beta V_0 = 1, 2, 4$, and ∞ . To emphasize the variation with βV_0 , the variable $Y \equiv \lambda_{\infty}/kv_0$ has been held constant rather than y [$\lambda_{\infty} \equiv \lambda_0(\beta V_0 \rightarrow \infty)$]. As expected, larger βV_0 yields a narrower line shape. Figure 9 shows the effect of the optimization on λ^* as a function of βV_0 .

It has been observed that $S_s(k, \omega)$, or $\mathcal{R}(x, y)$, is not sensitive to the intermolecular potential beyond the differences reflected through the diffusion coefficient.⁹ This is rigorously true of the usual $N=2$ model since in that case $\lambda^* = -1$ and $\mathcal{R}(x, y)$ has the universal form,

$$[\mathcal{R}(x, y)]_{N=2} = 2\text{Re}\{\phi(x + iy)/[i + y\phi(x + iy)]\} . \quad (4.12)$$

The potential form has been completely eliminated from (4.12) by the choice of dimensionless vari-

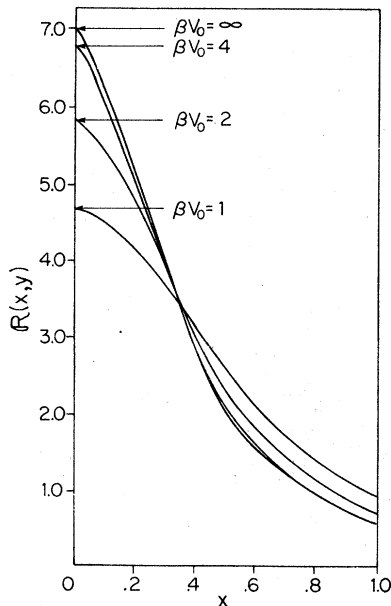


FIG. 8. $R(x, y)$ for Boltzmann step-potential kinetic equation for several values of the potential strength βV_0 , $\alpha + Y = 1.46$.

able, $y \equiv v_0/2Dk$ [Eq. (2.39)]. More generally, any additional dependence of $R(x, y)$ on the potential must occur through $\lambda^*(x, y)$. Figure 10 is the same plot of λ^* as in Fig. 9 except with y as a variable rather than Y . Clearly, most of the βV_0 dependence has been removed in this way, except at small y . However, at small y , collisions are dominated by free streaming so that the contribution to $R(x, y)$ from λ^* is lessened. Consequently, it is expected

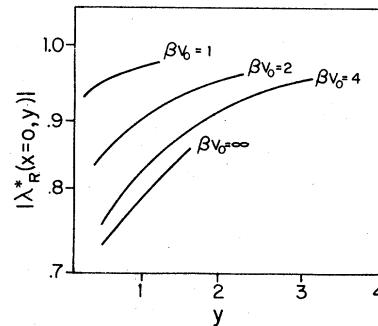


FIG. 10. Real part of $\lambda^*(x, y)$ for several values of βV_0 as a function of $y = v_0/2Dk$ (Boltzmann step potential).

that $R(x, y)$ is even less sensitive to variations in potential parameters than λ^* . Figure 11 shows the halfwidths for $\beta V_0 = 1, 2, 4$, and ∞ . While there is not much variation with βV_0 there is a noticeable trend for the halfwidths to approach a limiting form (the broken curve in Fig. 11) defined by the halfwidths associated with (4.12). This may be understood as follows. As βV_0 decreases, all matrix elements of M_B tend toward zero; in particular, $\lambda_0 \rightarrow 0$ as $\beta V_0 \rightarrow 0$. Therefore, decreasing βV_0 at constant y requires decreasing k and it is then easily verified that

$$\lim_{\beta V_0 \rightarrow 0} \lambda^* = -1$$

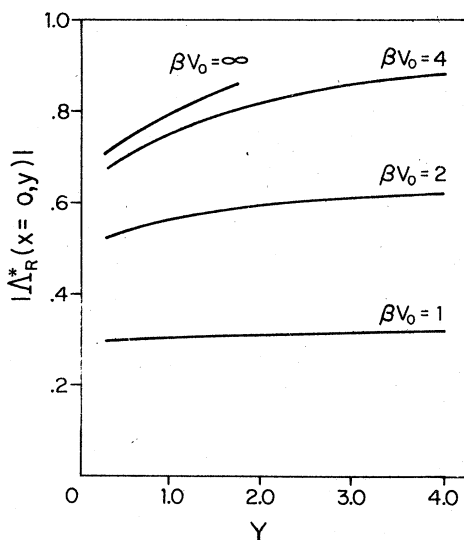


FIG. 9. Real part of $\Lambda^*(x, Y) \equiv \lambda^*(x, y)$ for several values of βV_0 as a function of $Y \equiv \lambda \infty/kv_0$ (Boltzmann step potential).

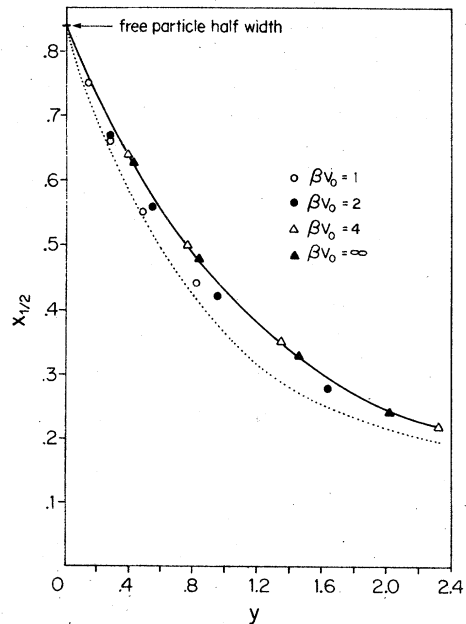


FIG. 11. Halfwidth at half maximum for $R(x, y)$ from the Boltzmann step-potential kinetic equation for $\beta V_0 = 1, 2, 4$, and ∞ . The $N=2$ Gross-Jackson model is also shown (\cdots) as the limiting case $\beta V_0 \rightarrow 0$, Eq. (4.13).

and consequently

$$\lim_{\beta V_0 \rightarrow 0} \mathcal{R}(x, y) \Big|_{y=\text{const.}} = 2\text{Re} \left(\frac{\phi(x+iy)}{i+y\phi(x+iy)} \right). \quad (4.13)$$

In Fig. 11, if both βV_0 and hard-core diameter were varied in such a way as to maintain constant collision frequency it may be expected that no significant changes in the halfwidths would be observed. For the same reasons, no discernible difference between, e.g., Lennard-Jones, hard sphere, and step potential is expected as long as the potential parameters all lead to collision frequencies of comparable size.

B. Finite-collision-time effects

Quite generally, apart from hard-sphere systems, the collision operator itself depends on k and ω . This occurs for the step potential through the contribution from ΔM , and arises as a consequence of the fact that the centers of the colliding pair are separated by a distance of the order of the scattering length and that finite times are required to complete a collision. For large k and ω the collisional details over small space and time scales, respectively, become important for the correct determination of matrix elements of M_s . However, for a dilute gas these variations occur at such large values of k and ω that they would be very difficult to detect in the structure of $\mathcal{R}(x, y)$. To see this, consider the order of magnitude of the k and ω dependence of ΔM from Eq. (4.5). The controlling factors are $1 - \exp[i(\omega - \vec{k} \cdot \vec{v})T]$ and $1 - \exp[i(\omega$

$-\vec{k} \cdot \vec{v})T$]. From Appendix A, T and T'' are of the order of magnitude of σ/v_0 , the average collision time. Thus the ω and k dependence will be important if $\omega\sigma/v_0 \geq 1$ and $k\sigma \geq 1$. Now consider the order of magnitude of the collision frequency λ_0 in a dilute gas. Typically, $\lambda_0 \sim n\pi\sigma^2 v_0$, where $\pi\sigma^2$ is an estimate of the cross section. The variables x and y may be written

$$x = \omega/kv_0 = (\omega\sigma/v_0)/k\sigma, \\ y = \lambda_0/kv_0 \sim (\pi\rho^*)(1/k\sigma),$$

where $\rho^* \equiv n\sigma^3$. Consider first the k dependence. If $k\sigma \geq 1$ then $y \lesssim \pi\rho^*$. But for a dilute gas $\rho^* \sim 10^{-2}$ so $y \lesssim \pi \times 10^{-2}$, i.e., $\mathcal{R}(x, y)$ is effectively independent of the collisions regardless of their k dependence. Similarly, from the above, $x \sim (\omega\sigma/v_0)(y/\pi\rho^*)$. If $\omega\sigma/v_0 \geq 1$ and y is of the order of 1, then $x \gtrsim (\pi\rho^*)^{-1}$, or $x \gtrsim \pi^{-1} \times 10^2$. This corresponds to a region far out in the wings where $\mathcal{R}(x, y)$ has decreased many orders of magnitude. We conclude then that while the k and ω dependence of M_s exists and (as will be shown below) is important for the determination of M , this dependence is not reflected in $\mathcal{R}(x, y)$ for dilute gases. The collision frequency is considerably larger for dense gases and liquids, however, and these effects become more significant for neutron scattering.

A convenient way to discuss the k and ω dependence of M_{sp} is to define the associated equilibrium collision frequency, i.e., the contribution from the terms involving only the unscattered velocity in Eqs. (4.4) and (4.5) [with $h(\vec{v}) = 1$]:

$$\nu(\vec{k}, \omega, \vec{v}) \equiv n\sigma^2 \int d\vec{v}_2 \phi(v_2) \int d\Omega (\hat{r} \cdot \vec{g}) \theta(\hat{r} \cdot \vec{g}) \{1 + e^{-\beta V_0} - e^{-\beta V_0} \exp[i(\omega - \vec{k} \cdot \vec{v})(2\sigma/g^2)\hat{r} \cdot \vec{g}]\}. \quad (4.14)$$

This may be written

$$\nu(\vec{k}, \omega, \vec{v}) = (1 + e^{-\beta V_0})\nu_B(v) - e^{-\beta V_0}\mu(\vec{k}, \omega, \vec{v}), \quad (4.15)$$

where $\nu_B(v)$ is the usual Boltzmann frequency

$$\nu_B(v) = n\sigma^2 \int d\vec{v}_2 \phi(v_2) \int d\Omega (\hat{r} \cdot \vec{g}) \theta(\hat{r} \cdot \vec{g}) \quad (4.16)$$

and the frequency-dependent term is

$$\mu(\vec{k}, \omega, \vec{v}) = n\sigma^2 \int d\vec{v}_2 \phi(v_2) \\ \times \int d\Omega (\hat{r} \cdot \vec{g}) \theta(\hat{r} \cdot \vec{g}) \\ \times \exp[i(\omega - \vec{k} \cdot \vec{v})(2\sigma/g^2)\hat{r} \cdot \vec{g}]. \quad (4.17)$$

These integrals may be readily reduced to

$$\nu_B(v) = \frac{1}{2}\nu_0 \left(e^{-\xi^2} + (1/\xi + 2\xi) \int_0^\xi dp e^{-p^2} \right), \quad (4.18)$$

$$\mu(\vec{k}, \omega, \vec{v}) = \frac{2\nu_0}{\xi\alpha^2} e^{-\xi^2} \int_0^\infty dp e^{-p^2} p^4 \sinh 2p\xi \\ \times [1 - (1 - i\alpha/p)e^{i\alpha/p}], \quad (4.19)$$

where $\xi \equiv \vec{v}/v_0$, $\nu_0 \equiv \nu_B(v=0) = 2\sqrt{\pi} n\sigma^2 v_0$, and

$$\alpha = (2\sigma/v_0)(\omega - \vec{k} \cdot \vec{v}) = (2\sigma\lambda_0/v_0 y)(x - \hat{k} \cdot \xi). \quad (4.20)$$

The integrals (4.18) and (4.19) have been computed numerically to determine $\nu(\vec{k}, \omega, \vec{v})$ as a function of the dimensionless quantities α and ξ . Figure 12 shows the variation of the real and imaginary parts of $\nu(\vec{k}, \omega, \vec{v})$ relative to the Boltzmann collision frequency for $\beta V_0 = 1$ and several values of ξ . Figure 13 shows the same quantities at $\xi = 1$ for βV_0

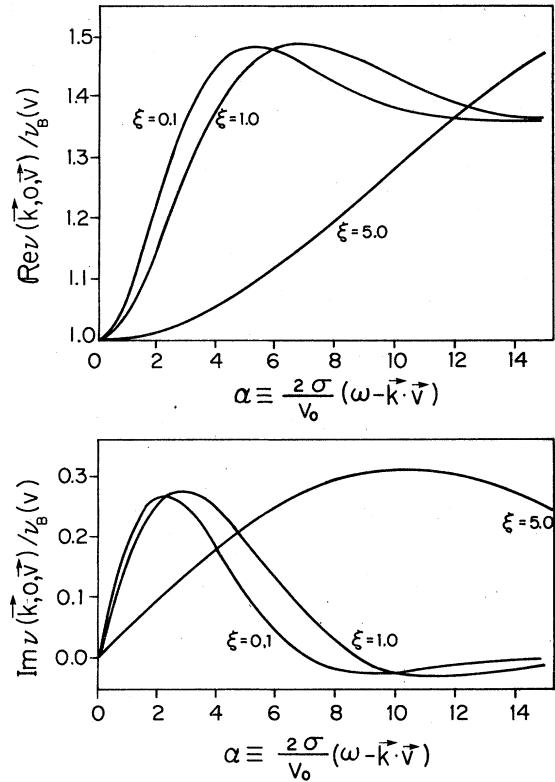


FIG. 12. Real and imaginary parts of the collision frequency relative to the Boltzmann collision frequency for several values of the relative velocity at $\beta V_0 = 1$.

$= 1, 2, 3$. The increase of $\nu(\vec{k}, \omega, \vec{v})$ over the Boltzmann value may be understood as follows. For low frequencies, corresponding to dynamics on a long-time scale, partial collisions of the type shown in Fig. 7(b) do not occur since there has been sufficient time to convert them to completed collisions. Similarly, the partial collisions of the type in Fig. 7(e) vanish due to a cancellation, after a time greater than a collision time, of contribu-

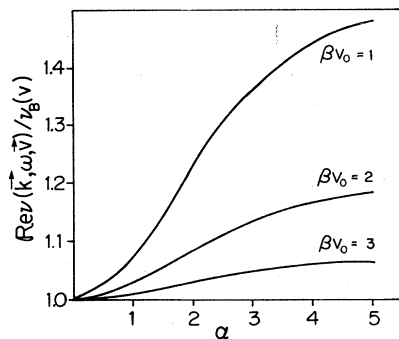


FIG. 13. Real part of the collision frequency relative to the Boltzmann collision frequency for several values of βV_0 at $\xi = 1$.

tions arising from particles initially inside the well, but on the opposite hemisphere [Fig. 7(c)]. As the frequency increases some of the completed collisions transform to partial collisions, but additionally the partial collisions of the types in Figs. 7(c) and 7(e) no longer cancel. Instead, the partial collisions are counted as being among those whose momentum has changed in a time $\Delta t \sim \omega^{-1}$. Equivalently, more phase space contributes to the number of particles changing momentum over a short time interval since initially overlapping particles contribute. These additional collisions may be estimated by counting the number of overlapping particles escaping through a hemisphere per unit time and area,

$$\Delta \nu \sim e^{-\beta V_0} \nu_B(v).$$

The factor $e^{-\beta V_0}$ comes from the decreased probability of overlap due to the repulsive potential and $\nu_B(v)$ arises from the estimate that the rate of collisions is equal to the rate at which overlaps separate. Thus

$$\text{Re}[\nu(\vec{k}, \omega, \vec{v}) / \nu_B(v)] \Big|_{\alpha \gg 1} \sim 1 + e^{-\beta V_0}$$

which is in substantial agreement with Fig. 13. The velocity dependence of Fig. 12 simply reflects the actual collision time decreases for increasing velocity so that the occurrence of partial collisions occur at correspondingly higher frequencies.

V. DISCUSSION

The optimization scheme discussed in Sec. II, specifically Eqs. (2.30) and (2.31) for the self-correlation function, is seen to provide substantial improvement over lowest-order kinetic modeling for several kinetic equations. Although the kinetic equations considered here are relatively simple, the collision operations (aside from the Fokker-Planck operation) are quite complex mathematically and probably provide adequate tests of the scheme under quite general conditions. It should be clear that there is a great deal of flexibility associated with the expansion (2.9) and choice of reference collision operator. For example, in discussion of mode-coupling corrections to the collision operator one might choose ΔM to consist of only such terms, and evaluate the reference fluid [i.e., R_N in Eq. (2.11)] using the optimized $N = 2$ Gross-Jackson model with λ^* determined without the mode-coupling effects. Other density effects might be treated in this way using the Enskog model as a reference.

Although the discussion of Sec. II included the modeling for $S(k, \omega)$, the calculations presented here were limited to those for the self-structure factor. The main difficulty for calculation of $S(k, \omega)$ lies in the fact that the hydrodynamic sub-

space is five dimensional for that case, and there is considerably more algebraic complexity in the expressions for λ^* . However, this is not a significant problem beyond the fact that all hydrodynamic matrix elements of M must be provided and for general k - and ω -dependent collision operators these are known only for the Enskog operator. Even for the step potential discussed in Sec. IV the k and ω dependence is quite difficult to obtain. We hope to discuss this problem elsewhere.

Regarding the results for the Boltzmann equation for the step potential, perhaps the most significant points are reflected in Fig. 11. Here it is clear that much of the dependence of $S_s(k, \omega)$ on the potential may be removed by scaling k to Dk where D is the self-diffusion coefficient. Consequently, $S_s(k, \omega)$ does not provide easy access to information not already contained in D . However, as Fig. 11 shows, there is a measurable residual difference between the halfwidth scaled this way for $\beta V_0 = 0$ (dotted line) and $\beta V_0 \rightarrow \infty$ (solid line), so that different potential models can be distinguished beyond their associated self-diffusion coefficients in so far as the potential strength, or more specifically the collision rates, differ. Such differentiation would be enhanced by the inclusion of the k dependence of the collision operator. As indicated in Sec. IV, however, at low density the k and ω dependence of the collision operator only affects the shape of $S_s(k, \omega)$ in the far wings. At higher densities these modifications should become more manifest.

ACKNOWLEDGMENTS

We wish to thank Professor Sidney Yip for providing the results of his $N = 35$ Gross-Jackson kinetic model for hard spheres, and for several helpful comments. Research was supported by the NSF under Grant No. PHY 76-21453.

APPENDIX A: LOW-DENSITY KINETIC EQUATION

The low-density kinetic equation may be obtained directly from a cluster expansion of the collision operator. The s cluster defines contributions to the collision operator from a correlated or interacting group of s particles with relative contribution of the order $(n\sigma^3)^{s-1}$. The cluster expansion, therefore, generates a formal series for the collision operator in powers of the density. The series is only formal since it is known that there are divergent parts from each s cluster for $s > 3$ (in three dimensions). However, there has been substantial study of the rearrangement of this series necessary for the removal of these divergencies and in all cases the contributions from $s \leq 3$ are unchanged and still dominate at sufficiently low density. While there is no rigorous proof of this

fact we shall assume here that the lowest-order cluster contribution does, in fact, define the low-density limit of the collision operator, independent of any rearrangement of the higher-order terms in the density expansion. There is one other point of caution, however, regarding the uniformity of this low-density limit with respect to time. The coupling of macroscopic (hydrodynamic) modes can yield contributions on a long time scale not present in the low-order cluster expansion. However, at low density these contributions are very small and occur on a time scale much too large to be observed by neutron or even light scattering.

The cluster expansion for kinetic equations is well described elsewhere,¹⁵ and the derivation leading to the low-density kinetic equation will only be sketched briefly here. More detail will be given to the reduction of the formal low-density equation for the step potential to a form suitable for calculation, to illustrate both the simplifications and care required in using discontinuous potentials. Only the kinetic equation for self-correlations will be considered.

A. Low-density kinetic equation

The self-structure factor $S_s(k, \omega)$ is defined in terms of a correlation in a way similar to Eq. (1.1) for $S(k, \omega)$,

$$S_s(k, \omega) = 2\text{Re} F_s(k, \omega),$$

$$F_s(k, \omega) = \int_0^\infty dt e^{i\omega t} \int d\vec{r} e^{-i\vec{k}\cdot\vec{r}} \times \frac{N}{n} \langle \delta(\vec{r} - \vec{q}_1(t)) \delta(\vec{q}_1(0)) \rangle \quad (\text{A1})$$

where $\vec{q}_1(0)$ and $\vec{q}_1(t)$ are the positions of particle 1 at times 0 and t , respectively, and N is the total number of particles. The expression for $F_s(k, \omega)$ may be written

$$F_s(k, \omega) = \int dx_1 e^{-i\vec{k}\cdot\vec{q}_1} \tilde{\psi}^{(1)}(x_1, \omega), \quad (\text{A2})$$

where x_1 denotes the position and momentum of particle 1. Also, $\tilde{\psi}^{(1)}(x_1, \omega)$ is the first member of a set of functions defined by

$$n^s \tilde{\psi}^{(s)}(x_1 \cdots x_s; \omega) \equiv \int_0^\infty dt e^{i\omega t} \frac{N!}{(N-s)!} \times \int dx_{s+1} \cdots dx_N \rho_0 \delta(\vec{q}_1(-t)), \quad (\text{A3})$$

where ρ_0 is the equilibrium canonical distribution function. The time dependence of the δ function may be represented by

$$\delta(\vec{q}_1(-t)) = e^{-L N t} \delta(\vec{q}_1),$$

where L_N is the Liouville operator for the system. Equation (A3) may then be written in the suggestive form

$$n^s \tilde{\psi}^{(s)}(x_1 \cdots x_s; \omega) \equiv \tilde{U}(x_1 \cdots x_s; \omega) \delta(\vec{q}_1) \quad (\text{A4})$$

with the operators, $\tilde{U}(x_1 \cdots x_s; \omega)$, defined by

$$\begin{aligned} \tilde{U}(x_1, \dots, x_s; \omega) &\equiv \int_0^\infty dt e^{i\omega t} U(x_1, \dots, x_s; t), \\ U(x_1, \dots, x_s; t) &\equiv \frac{N!}{(N-s)!} \int dx_{s+1} \cdots dx_N W(x_1, \dots, x_N; t), \\ W(x_1, \dots, x_N; t) &\equiv \rho_0 e^{-L_N t}. \end{aligned} \quad (\text{A5})$$

The collision operator may now be defined in terms of the \tilde{U} operators as follows. The functions $\tilde{\psi}^{(s)}$ satisfy the Laplace transformed Bogoliubov-Born-Green-Kirkwood-Yvon (BBGKY) hierarchy of equations, the first one of which is

$$(-i\omega + \vec{v}_1 \cdot \vec{\nabla}_1) \tilde{\psi}^{(1)} - n \int dx_2 \theta_{12} \tilde{\psi}^{(2)} = \phi(p_1) \delta(\vec{q}_1). \quad (\text{A6})$$

Here $\phi(p)$ is the Maxwell-Boltzmann distribution and θ_{12} is defined by

$$\theta_{12} \equiv [\vec{\nabla}_{r_{12}} V(r_{12})] \cdot (\vec{\nabla}_{p_1} - \vec{\nabla}_{p_2}) \quad (\text{A7})$$

and $V(r_{12})$ is the intermolecular potential at sep-

$$(-i\omega + i\vec{k} \cdot \vec{v} - M_s) h(\vec{k}, \omega, \vec{v}) = 1, \quad (\text{A12})$$

$$M_s[h] \equiv \phi^{-1}(p_1) \int d\vec{q}_1 e^{-i\vec{k} \cdot \vec{q}_1} \int \frac{d\vec{k}'}{(2\pi)^3} \int dx_2 \theta_{12} \tilde{U}(x_1, x_2; \omega) \tilde{U}^{-1}(x_1; \omega) \phi(p_1) e^{i\vec{k} \cdot \vec{q}_1} h(\vec{k}', \omega, \vec{v}_1). \quad (\text{A13})$$

The results (A11)–(A13) are formally exact for liquids as well as gases. To obtain the explicit form of M_s for low density we need only the leading term in the cluster expansion of $\tilde{U}(x_1, x_2; \omega)$ and $\tilde{U}^{-1}(x_1; \omega)$,

$$\tilde{U}(x_1; \omega) = \int_0^\infty dt e^{i\omega t} n \phi(p_1) e^{-L(1)t}, \quad (\text{A14})$$

$$\tilde{U}(x_1, x_2; \omega) = \int_0^\infty dt e^{i\omega t} n^2 \phi(p_1) \phi(p_2) e^{-\mathcal{G} \nu(r_{12})} e^{-L(12)t}.$$

Here $L(1)$ and $L(12)$ are the one- and two-particle Liouville operators. Carrying out the integration in (A14) and substitution into (A13) gives the low-density form of the collision operator

$$M_s[h] \xrightarrow{\text{low density}} n \phi^{-1}(p_1) \int d\vec{q}_1 e^{-i\vec{k} \cdot \vec{q}_1} \int \frac{d\vec{k}'}{(2\pi)^3} \int dx_2 \theta_{12} \phi(p_1) \phi(p_2) e^{-\mathcal{G} \nu(r_{12})} \mathcal{G}(1, 2; \omega) \mathcal{G}_0^{-1}(1, 2; \omega) e^{i\vec{k} \cdot \vec{q}_1} h(\vec{k}', \omega, \vec{v}_1) \quad (\text{A15})$$

with

$$\mathcal{G}(1, 2; \omega) \equiv [-i\omega + L(1, 2)]^{-1},$$

$$\mathcal{G}_0(1, 2; \omega) \equiv [-i\omega + L_0(1, 2)]^{-1},$$

$$L(1, 2) \equiv L_0(1, 2) - \theta_{12},$$

and $L_0(1, 2)$ is the two-particle Liouville operator for noninteracting particles. Introducing relative and center-of-mass coordinates

aration $\vec{r}_{12} \equiv \vec{q}_1 - \vec{q}_2$. This form of θ_{12} assumes a continuous (and differentiable) potential; however, the derivation holds for discontinuous potentials as well with suitable modification of θ_{12} . The kinetic equation is a closed equation which follows from (A6) once $\tilde{\psi}^{(2)}$ is expressed in terms of $\tilde{\psi}^{(1)}$. This may be done formally by considering equations (A4) for $s=1, 2$ and eliminating $\delta(\vec{q}_1)$ between them, i.e.,

$$n \tilde{\psi}^{(2)}(x_1, x_2; \omega) = \tilde{U}(x_1, x_2; \omega) \tilde{U}^{-1}(x_1; \omega) \tilde{\psi}^{(1)}(x_1; \omega). \quad (\text{A8})$$

Substitution into (A6) then gives the desired kinetic equation

$$\begin{aligned} (-i\omega + \vec{v}_1 \cdot \vec{\nabla}_1) \tilde{\psi}^{(1)} - \int dx_2 \theta_{12} \tilde{U}(x_1, x_2; \omega) \\ \times \tilde{U}^{-1}(x_1; \omega) \tilde{\psi}^{(1)} = \phi(p_1) \delta(\vec{q}_1). \end{aligned} \quad (\text{A9})$$

This equation may be written in the notation of the text by defining

$$h(\vec{k}, \omega, \vec{v}_1) \equiv \phi^{-1}(p_1) \int d\vec{q}_1 e^{-i\vec{k} \cdot \vec{q}_1} \tilde{\psi}^{(1)}(x_1; \omega) \quad (\text{A10})$$

so that Eqs. (A1) and (A2) become

$$S_s(h, \omega) = 2\text{Re}(1, h) \quad (\text{A11})$$

and h satisfies the kinetic equation

$$\vec{r} \equiv \vec{r}_{21} \equiv \vec{q}_2 - \vec{q}_1, \quad \vec{R} \equiv \frac{1}{2}(\vec{q}_1 + \vec{q}_2)$$

$$\vec{g} \equiv \vec{v}_2 - \vec{v}_1, \quad \vec{V} \equiv \frac{1}{2}(\vec{v}_1 + \vec{v}_2)$$

and using the identity

$$\theta_{12} \phi(p_1) \phi(p_2) e^{-\mathcal{G} \nu(r_{12})} \mathcal{G} = \mathcal{G}_0^{-1} [\mathcal{G} - \mathcal{G}_0] \phi(p_1) \phi(p_2) e^{-\mathcal{G} \nu(r_{12})}$$

then gives

$$\begin{aligned}
M_s[h] &= n \phi^{-1}(p_1) \int \frac{d\vec{k}'}{(2\pi)^3} \int d\vec{r} d\vec{R} d\vec{p}_2 e^{-i\vec{k}\cdot\vec{R}} e^{i\vec{k}\cdot\vec{r}/2} \mathcal{G}_0^{-1} [\mathcal{G} - \mathcal{G}_0] \phi(p_1) \phi(p_2) e^{-\mathcal{B}V(r)} \mathcal{G}_0^{-1} e^{i\vec{k}\cdot\vec{R}} e^{-i\vec{k}\cdot\vec{r}/2} h(\vec{k}', \omega, \vec{v}_1) \\
&= n \phi^{-1}(p_1) \int_0^\infty dt e^{t\omega t} \int \frac{d\vec{k}'}{(2\pi)^3} \int d\vec{r} d\vec{R} d\vec{p}_2 e^{-i\vec{k}\cdot\vec{R}} e^{i\vec{k}\cdot\vec{r}/2} \mathcal{G}_0^{-1} \\
&\quad \times (e^{-L(1)2t} - e^{-L_0(1)2t}) \phi(p_1) \phi(p_2) e^{-\mathcal{B}V(r)} \mathcal{G}_0^{-1} \exp(i\vec{k}'\cdot\vec{R} - i\vec{k}'\cdot\vec{r}/2) h(\vec{k}', \omega, \vec{v}_1) \\
&= n \phi^{-1}(p_1) \int_0^\infty dt e^{t\omega t} \int d\vec{p}_2 d\vec{r} \exp(i\vec{k}\cdot\vec{r}/2 - i\vec{k}\cdot\vec{V}t) (-i\omega + i\vec{k}\cdot\vec{V} + \vec{g}\cdot\vec{\nabla}_r) (e^{-\vec{L}\vec{r}, \vec{g}t} - e^{-\vec{L}_0\vec{r}, \vec{g}t}) \\
&\quad \times \phi(p_1) \phi(p_2) e^{-\mathcal{B}V(r)} (-i\omega + i\vec{k}\cdot\vec{V} - \frac{1}{2}i\vec{k}\cdot\vec{g}) e^{-i\vec{k}\cdot\vec{r}/2} h(\vec{k}, \omega, \vec{v}_1) \\
&= n \int_0^\infty dt e^{t\omega t} \int d\vec{p}_2 \phi(p_2) e^{-i\vec{k}\cdot\vec{v}t} \int d\vec{r} e^{i\vec{k}\cdot\vec{r}/2} (-i\omega + i\vec{k}\cdot\vec{V} + \vec{g}\cdot\vec{\nabla}_r) \\
&\quad \times (e^{-\mathcal{B}V(r)} e^{-\vec{L}t} - e^{-\vec{L}_0t} e^{-\mathcal{B}V(r)}) e^{-i\vec{k}\cdot\vec{r}/2} (-i\omega + i\vec{k}\cdot\vec{V} - \frac{1}{2}i\vec{k}\cdot\vec{g}) h(\vec{k}, \omega, \vec{v}_1); \\
M_s[h] &= n \int_0^\infty dt e^{t\omega t} \int d\vec{p}_2 \phi(p_2) e^{-i\vec{k}\cdot\vec{v}t} \int d\vec{r} \vec{g}\cdot\vec{\nabla}_r e^{i\vec{k}\cdot\vec{r}/2} \\
&\quad \times (e^{-\mathcal{B}V(r)} e^{-\vec{L}t} - e^{-\vec{L}_0t} e^{-\mathcal{B}V(r)}) e^{-i\vec{k}\cdot\vec{r}/2} \mathcal{G}_0^{-1}(\vec{k}, \omega) h(\vec{k}, \omega, \vec{v}_1) \\
&\quad + n \int_0^\infty dt e^{t\omega t} \int d\vec{p}_2 \phi(p_2) e^{-i\vec{k}\cdot\vec{v}t} \mathcal{G}_0^{-1}(\vec{k}, \omega) \int d\vec{r} e^{i\vec{k}\cdot\vec{r}/2} (e^{-\mathcal{B}V(r)} e^{-\vec{L}t} - e^{-\vec{L}_0t} e^{-\mathcal{B}V(r)}) e^{-i\vec{k}\cdot\vec{r}/2} \mathcal{G}_0^{-1} h(\vec{k}, \omega, \vec{v}_1), \quad (A16)
\end{aligned}$$

where

$$\mathcal{G}_0(\vec{k}, \omega) = (-i\omega + i\vec{k}\cdot\vec{V} - \frac{1}{2}i\vec{k}\cdot\vec{g})^{-1},$$

$$\vec{L}_0(\vec{r}, \vec{g}) = \vec{g}\cdot\vec{\nabla}_r,$$

$$\vec{L}(\vec{r}, \vec{g}) = \vec{g}\cdot\vec{\nabla}_r - (2/m)[\vec{\nabla}_r V(r)]\cdot\vec{\nabla}_r.$$

Also \vec{V} and \vec{g} are the center of mass and relative velocities, respectively. The results (A15) or (A16) apply for an arbitrary central potential; however, the form (A16) makes no explicit reference to the force law except through $e^{-\vec{L}t}$ and is therefore convenient for the discussion of discontinuous potentials.

B. Reduction of $M_s(k, \omega)$ for the step potential

To simplify Eq. (A16) consider the case of a step potential. This may be defined as the limit of a continuous potentials.

$$\begin{aligned}
M_s[h] &= \lim_{\epsilon \rightarrow 0} n \int_0^\infty dt e^{t\omega t} \int d\vec{p}_2 \phi(p_2) e^{-i\vec{k}\cdot\vec{v}t} \int d\Omega \hat{r}\cdot\vec{g} \int_{\sigma-\epsilon/2}^{\sigma+\epsilon/2} dr r^2 \frac{d}{dr} e^{i\vec{k}\cdot\vec{r}/2} (e^{-\mathcal{B}V(r)} e^{-\vec{L}t} - e^{-\vec{L}_0t} e^{-\mathcal{B}V(r)}) \\
&\quad \times e^{-i\vec{k}\cdot\vec{r}/2} \mathcal{G}_0^{-1}(\vec{k}, \omega) h(\vec{k}, \omega, \vec{v}_1). \quad (A17)
\end{aligned}$$

The free streaming part of M_s in (A17) may be written as

$$M_s^{fs}[h] = -n\sigma^2 \int_0^\infty dt e^{t\omega t} \int d\vec{v}_2 \phi(v_2) e^{-i\vec{k}\cdot\vec{v}t} \int d\Omega (\hat{r}\cdot\vec{g}) [\{e^{-\mathcal{B}V(\vec{r}-\vec{z}t)} e^{i\vec{k}\cdot\vec{z}t/2} (-i\omega + i\vec{k}\cdot\vec{V} - i\vec{k}\cdot\vec{g}/2) h(\vec{V}, \vec{g})\}_{\sigma_+} - \{ \}_{\sigma_-}]. \quad (A18)$$

The difference of the two curly brackets is only nonzero and finite for an infinitesimal period of time and therefore M_s^{fs} doesn't contribute. A transformation $\hat{r} \rightarrow -\hat{r}$ brings the time propagation for

$$V(\epsilon, r) \equiv \begin{cases} V_0, & r < \sigma - \frac{1}{2}\epsilon \\ -(V_0/\epsilon)(r - \sigma - \frac{1}{2}\epsilon), & \sigma - \frac{1}{2}\epsilon < r < \sigma + \frac{1}{2}\epsilon \\ 0, & r > \sigma + \frac{1}{2}\epsilon \end{cases}$$

as $\epsilon \rightarrow 0$. Now the r integration in the second term of M_s above is

$$\int_{\sigma-\epsilon/2}^{\sigma+\epsilon/2} dr r^2 e^{i\vec{k}\cdot\vec{r}/2} (e^{-\mathcal{B}V(r)} e^{-\vec{L}t} - e^{-\vec{L}_0t} e^{-\mathcal{B}V(r)}) \times e^{-i\vec{k}\cdot\vec{r}/2} \mathcal{G}_0^{-1}(\vec{k}, \omega) h(\vec{k}, \omega, \vec{v}_1).$$

The integrand is bounded and well behaved as $\epsilon \rightarrow 0$ so the integral vanishes as $\epsilon \rightarrow 0$ due to vanishing domain of integration. Hence the second term of M does not contribute for a step potential. However, the first term does not vanish, due to the presence of the $\vec{\nabla}_r$, which generates a singular integrand as $\epsilon \rightarrow 0$ by differentiating the discontinuous potential. Thus

particle trajectories into the positive direction, i.e.,

$$M_s[h] = -n\sigma \int_0^\infty dt e^{i\omega t} \int d\vec{v}_2 \phi(v_2) e^{-i\vec{k}\cdot\vec{v}t} \int d\Omega (\hat{r}\cdot\vec{g}) e^{-i\vec{k}\cdot\vec{r}/2} \times \{ [e^{-\beta V(r)} e^{i\vec{k}\cdot\vec{g}} e^{i\vec{k}\cdot\vec{r}/2} g_0^{-1} h(\vec{V}, \vec{g}) \}_{\sigma_+} - \{ \}_{\sigma_-} \}. \quad (\text{A19})$$

The first term represents collisions with particles initially noninteracting, while the second represents particles initially overlapping.

Consider the contributions to (A19) from the two hemispheres, $\hat{r}\cdot\vec{g} > 0$ (M^+) and $\hat{r}\cdot\vec{g} < 0$ (M^-). The collision dynamics for $\hat{r}\cdot\vec{g} > 0$ are displayed in Figs. 7(d) and 7(e). The contribution of (A19) to M^+ is readily reduced to

$$M^+[h] = -n\sigma^2 \int d\vec{v}_2 \phi(v_2) \int d\Omega \hat{r}\cdot\vec{g} \theta(\hat{r}\cdot\vec{g}) [h(\vec{V}, \vec{g}) - e^{-\beta V_0} h(\vec{V}, \vec{g}^*)]. \quad (\text{A20})$$

The trajectories for $\hat{r}\cdot\vec{g} < 0$ are shown in Figs. 7(a), 7(b), and 7(c). In the analysis of Figs. 7(b) and 7(c), two time intervals must be used. For example, in the contribution to M^- represented by Fig. 7(b), the time integral is broken up into the ranges $0 < t < T''$ and $T'' < t < \infty$. Also, for the part of M^- described by Fig. 7(c), the vector \hat{r} is transformed to the exit point \hat{r}^* . The scattered velocity \vec{g}^* , as a function of this new radial vector, is just \vec{g}^* of Fig. 7(b). Thus

$$\begin{aligned} M^-[h] = & -n\sigma^2 \int d\vec{v}_2 \phi(v_2) \int d\Omega (\hat{r}\cdot\vec{g}) \theta(-\hat{r}\cdot\vec{g}) \\ & \times [\theta(4V_0/m - (\hat{r}\cdot\vec{g})^2) h(\vec{V}, \vec{g}) \\ & + \theta((\hat{r}\cdot\vec{g})^2 - 4V_0/m) \{ f''(\vec{k}, \omega, \vec{g}, \hat{r}) h(\vec{V}, \vec{g}'') + [1 - f''(\vec{k}, \omega, \vec{g}, \hat{r})] h(\vec{V}, \vec{g}''') \}] \\ & - n\sigma^2 \int d\vec{v}_2 \phi(v_2) \int d\Omega (\hat{r}\cdot\vec{g}) \theta(\hat{r}\cdot\vec{g}) e^{-\beta V_0} \{ f(\vec{k}, \omega, \vec{g}, \hat{r}) h(\vec{V}, \vec{g}) + [1 - f(\vec{k}, \omega, \vec{g}, \hat{r})] h(\vec{V}, \vec{g}^*) \}, \\ f(\vec{k}, \omega, \vec{g}, \hat{r}) = & 1 - \exp[i(\omega - \vec{k}\cdot\vec{V} + \vec{k}\cdot\vec{g}/2)T(\vec{g}, \hat{r})], \\ f''(\vec{k}, \omega, \vec{g}, \hat{r}) = & 1 - \exp[i(\omega - \vec{k}\cdot\vec{V} + \vec{k}\cdot\vec{g}''/2)T''(\vec{g}, \hat{r})]. \end{aligned} \quad (\text{A21})$$

Combining (A20) and (A21) gives the desired result,

$$M_s[h] = M_B[h] + \Delta M[h],$$

where M_B is the Boltzmann limit form ($\hbar, \omega \rightarrow 0$),

$$\begin{aligned} M_B[h] = & -n\sigma^2 \int d\vec{v}_2 \phi(v_2) \int d\Omega (\hat{r}\cdot\vec{g}) \theta(-\hat{r}\cdot\vec{g}) \\ & \times \{ \theta(4V_0/m - (\hat{r}\cdot\vec{g})^2) [h(\vec{V}, \vec{g}') - h(\vec{V}, \vec{g})] + \theta((\hat{r}\cdot\vec{g})^2 - 4V_0/m) [h(\vec{V}, \vec{g}''') - h(\vec{V}, \vec{g})] \} \end{aligned} \quad (\text{A22})$$

and

$$\begin{aligned} \Delta M[h] = & -n\sigma^2 \int d\vec{v}_2 \phi(v_2) \int d\Omega (\hat{r}\cdot\vec{g}) \{ \theta(-\hat{r}\cdot\vec{g}) \theta((\hat{r}\cdot\vec{g})^2 - 4V_0/m) f''(\vec{k}, \omega, \vec{g}, \hat{r}) [h(\vec{V}, \vec{g}'') - h(\vec{V}, \vec{g}''')] \\ & - \theta(\hat{r}\cdot\vec{g}) e^{-\beta V_0} f(\vec{k}, \omega, \vec{g}, \hat{r}) [h(\vec{V}, \vec{g}^*) - h(\vec{V}, \vec{g})] \}. \end{aligned} \quad (\text{A23})$$

The scattered velocities in Fig. 7 are readily calculated from consideration of the two-body conservation laws and the geometry of the figure, with the results,

$$\begin{aligned}
\vec{g}' &= \vec{g} - 2\hat{r}g(\hat{g}\cdot\hat{r}), \\
\vec{g}'' &= \vec{g} - \hat{r}g(\hat{g}\cdot\hat{r} + a_2), \\
\vec{g}''' &= \vec{g}'' - \hat{r}''g''\{\hat{g}''\cdot\hat{r}'' - [(\hat{g}''\cdot\hat{r}'')^2 + 4V_0/mg''^2]^{1/2}\} \\
&= \vec{g}''[1 - (2a_2/a_1^2)(\hat{g}\cdot\hat{r} + a_2)] \\
&\quad - 2\hat{r}g[\hat{g}\cdot\hat{r} + a_2][1 - (a_2/a_1)(\hat{g}\cdot\hat{r} + a_2)] \quad (A24)
\end{aligned}$$

$$\vec{g}^* = \vec{g} - \hat{r}g(\hat{g}\cdot\hat{r} - a_3),$$

$$a_1^2 = 1 - \frac{4V_0}{mg^2}; \quad a_2^2 = (\hat{g}\cdot\hat{r})^2 - \frac{4V_0}{mg^2};$$

$$a_3^2 = (\hat{g}\cdot\hat{r})^2 + \frac{4V_0}{mg^2};$$

$$T = 2\sigma|\hat{g}\cdot\hat{r}|/g, \quad T'' = 2\sigma a_2/ga_1^2.$$

Equations (A11), (A12), (A22), and (A23) define the exact low-density kinetic theory of the self-structure factor for step-potential interaction used in Sec. IV.

$$A_{sp} = [(kv_0)^2/2\lambda_0](G^*, M_B G) = A_1 + A_2,$$

$$A_1 = + \frac{n(\sigma kv_0)^2}{2\lambda_0} \int d\vec{v} \phi(v) \int d\vec{v}_2 \phi(v_2) \int d\Omega (\hat{r}\cdot\vec{g})\theta(-\hat{r}\cdot\vec{g})(-i\omega + i\vec{k}\cdot\vec{V} - \frac{1}{2}i\vec{k}\cdot\vec{g} - \lambda)^{-2},$$

$$A_2 = - \frac{n(\sigma kv_0)^2}{2\lambda_0} \int d\vec{v} \phi(v) \int d\vec{v}_2 \phi(v_2) \int d\Omega (\hat{r}\cdot\vec{g})\theta(-\hat{r}\cdot\vec{g})(-i\omega + i\vec{k}\cdot\vec{V} - \frac{1}{2}i\vec{k}\cdot\vec{g} - \lambda)^{-1}$$

$$\times [\theta(4V_0/m - (\hat{r}\cdot\vec{g})^2)(-i\omega + i\vec{k}\cdot\vec{V} - \frac{1}{2}i\vec{k}\cdot\vec{g}' - \lambda)^{-1}$$

$$+ \theta((\hat{r}\cdot\vec{g})^2 - 4V_0/m)(-i\omega + i\vec{k}\cdot\vec{V} - \frac{1}{2}i\vec{k}\cdot\vec{g}''' - \lambda)^{-1}]. \quad (B1)$$

The contribution of A_1 will be evaluated first. The integrals over \vec{v} and \vec{v}_2 are transformed to the \vec{V} and \vec{g} of Appendix A. In terms of the variables of (2.33) and the dimensionless velocities,

$$\vec{U} = \sqrt{2}\vec{V}/v_0, \quad \vec{s} = \vec{g}/\sqrt{2}v_0; \quad (B2)$$

A_1 becomes

$$A_1 = \frac{3}{4\pi^{5/2}} \int d\vec{s} s e^{-s^2} \int d\vec{U} e^{-U^2} (\hat{k}\cdot\vec{U} - \hat{k}\cdot\vec{s} - \sqrt{2}z)^{-2}$$

$$\times \int_0^{2\pi} d\phi \int_0^\pi d\theta \sin\theta \cos\theta.$$

(B3)

The collision hemisphere integration is trivial. A few manipulations give,

$$A_2 = \frac{3}{4\pi^{5/2}} \int_{-\infty}^{\infty} dU e^{-U^2} \int d\vec{s} s e^{-s^2} (U - \hat{k}\cdot\vec{s} - \sqrt{2}z)^{-1} \int_0^{2\pi} d\phi \int_0^{\pi/2} d\theta \sin\theta$$

$$\times \cos\theta [\theta(\beta V_0 - s^2 \cos^2\theta)(U - \hat{k}\cdot\vec{s}' - \sqrt{2}z)^{-1} + \theta(s^2 \cos^2\theta - \beta V_0)(U - \hat{k}\cdot\vec{s}''' - \sqrt{2}z)^{-1}]. \quad (B6)$$

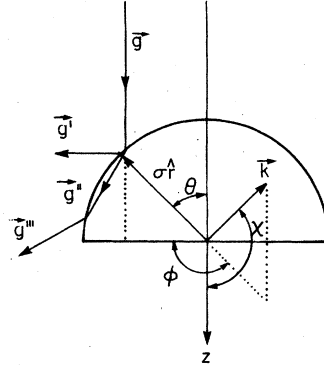


FIG. 14. Geometry of step-potential collisions for $\hat{r}\cdot\vec{g} < 0$.

APPENDIX B: STEP-POTENTIAL MODEL

In this section, the details of the reduction of the matrix element (4.9) with the step-potential Boltzmann operator will be shown. The matrix element is

$$\begin{aligned}
&\int d\vec{U} e^{-U^2} (F + \hat{k}\cdot\vec{U})^{-1} (F' + \hat{k}\cdot\vec{U})^{-1} \\
&= \pi \int_{-\infty}^{\infty} dU (F + U)^{-1} (F' + U)^{-1}, \quad (B4)
\end{aligned}$$

where F and F' do not depend on \vec{U} and may be equal to each other. Following the angular integration for \vec{s} is the result

$$A_1 = \frac{3}{\sqrt{\pi}} \int_{-\infty}^{\infty} dU e^{-U^2} \int_0^\infty ds s^3 e^{-s^2} \frac{1}{(U + \sqrt{2}z)^2 - s^2}. \quad (B5)$$

The reduction of A_2 is complicated by the coupling between the collision hemisphere and relative velocity integrals. The geometry of the two possible collisions for A_2 is shown in Fig. 14. Again the dimensionless variables in (B2) are introduced and the angular integration of \vec{U} is performed using (B4). At this point, A_2 is

To proceed further, the denominators in (B6) containing scattered velocities are expanded in Legendre polynomials, using (B14),

$$(U - \hat{k} \cdot \vec{s}' - \sqrt{2}z)^{-1} = \sum_{l=0}^{\infty} D_l(U, z, s) P_l(\hat{k} \cdot \hat{s}'),$$

$$D_l(U, z, s) = \frac{2l+1}{s} Q_l\left(\frac{U - \sqrt{2}z}{s}\right).$$
(B7)

An analogous equation exists for \vec{s}''' and since $s = s''' = s'$, the D_l coefficients are equal for the two types of collisions.

The expansion of (B7) is substituted into (B6). Next, the addition theorem,

$$P_l(\hat{k} \cdot \hat{s}') = P_l(\hat{k} \cdot \hat{s}) P_l(\hat{s} \cdot \hat{s}') + 2 \sum_{m=1}^l \frac{(l-m)!}{(l+m)!} P_l^m(\hat{k} \cdot \hat{s}) P_l^m(\hat{s} \cdot \hat{s}') \cos m\phi$$
(B8)

is used, for example, to eliminate the angle between \vec{s}' and \vec{k} in favor of the angle between \vec{s}' and \vec{s} . The sum in (B8) vanishes upon the ϕ integration, leaving,

$$A_2 = \frac{3}{2\pi^{3/2}} \int_{-\infty}^{\infty} dU e^{-U^2} \int d\vec{s} e^{-s^2} (U - \hat{k} \cdot \vec{s} - \sqrt{2}z)^{-1} \sum_{l=0}^{\infty} (2l+1) P_l(\hat{k} \cdot \hat{s})$$

$$\times Q_l\left(\frac{U - \sqrt{2}z}{s}\right) \int_0^{\pi/2} d\theta \sin\theta \cos\theta \{P_l(\hat{s} \cdot \hat{s}') + \theta(s^2 \cos^2\theta - \beta V_0)$$

$$[P_l(\hat{s} \cdot \hat{s}''') - P_l(\hat{s} \cdot \hat{s}')]\},$$
(B9)

where the hard-sphere part has been explicitly separated. From the formulas in (A24),

$$\hat{s} \cdot \hat{s}' = 1 - 2 \cos^2\theta,$$

$$\hat{s} \cdot \hat{s}''' = (2/a^2)[1 - \cos^2\theta + \cos\theta(\cos^2\theta - \beta V_0/s^2)^{1/2}]^2 - 1,$$

$$a^2 = 1 - \beta V_0/s^2.$$
(B10)

The angular \vec{s} integration is easily done using (B14)

identifying χ as the angle between \vec{s} and \vec{k} . The hard-sphere part of (B9) especially simplifies, using

$$\int_0^{\pi/2} d\theta \sin\theta (\cos\theta) P_l(1 - 2 \cos^2\theta) = \frac{1}{2} \delta_{l,0}.$$
(B11)

A transformation from θ to q , defined by $\cos^2\theta = 1 - qa^2$ is used to stretch the limits of the remaining angular integration in (B9). The result is

$$A_2 = -\frac{3}{\sqrt{\pi}} \int_{-\infty}^{\infty} du e^{-u^2} \int_0^{\infty} ds s e^{-s^2} \left[Q_0^2\left(\frac{u - \sqrt{2}z}{s}\right) + a^2 \theta(s^2 - \beta V_0) \sum_{l=0}^{\infty} (2l+1) Q_l^2\left(\frac{u - \sqrt{2}z}{s}\right) \right.$$

$$\times \int_0^1 dq \{P_l[2[qa + (1 - a^2q)^{1/2}(1 - q)^{1/2}]^2 - 1] - P_l(2a^2q - 1)\} \left. \right].$$
(B12)

Combining (B5) and (B12) leads to (4.11). The hard-sphere limit is obtained by neglecting the sum in (B12). It may be verified by a Laurent expansion in z of (3.11) and (3.12) that $\lim_{\beta V_0 \rightarrow 0} \lambda_{hs}^*(z) = -1$. It is also expected that the effects of collisions are negligible as $\beta V_0 \rightarrow 0$, and so $\lim_{\beta V_0 \rightarrow 0} \lambda_{sp}^* = 0$. In this limit, (4.11) becomes

$$\lim_{\beta V_0 \rightarrow 0} A_{sp}(z, \beta V_0) = \frac{3}{\sqrt{\pi}} \int_{-\infty}^{\infty} du e^{-u^2} \int_0^{\infty} ds s e^{-s^2} \left[\frac{s^2}{(u - \sqrt{2}z)^2 - s^2} - \sum_{l=0}^{\infty} (2l+1) Q_l^2\left(\frac{u - \sqrt{2}z}{s}\right) \right],$$
(B13)

which can be shown to be zero using

$$(z - \chi)^{-1} = \sum_{l=0}^{\infty} (2l+1) P_l(\chi) Q_l(z), \quad \int_{-1}^1 d\chi \frac{P_l(\chi)}{z - \chi} = 2Q_l(z).$$
(B14)

- *Present address, Dept. of Chemical Engineering, Tulane University, New Orleans, La. 70118.
- †Present address, Chemistry Dept., University of British Columbia, Vancouver, British Columbia.
- ¹P. A. Egelstaff, *Thermal Neutron Scattering* (Academic, New York, 1965), Chaps. 7 and 8; N. H. March and M. P. Tosi, *Atomic Dynamics in Liquids* (Halsted, New York, 1976).
- ²See, for example, P. Schofield, *Specialist Reports-Statistical Mechanics* (The Chemical Society, London, 1975).
- ³G. F. Mazenko, T. Y. Wei, and S. Yip, *Phys. Rev. A* **6**, 1981 (1972); A. Sugawara and S. Yip, *Phys. Fluids* **11**, 925 (1968).
- ⁴A preliminary report of this work is given by J. Dufty, L. Groome, K. Gubbins, and P. Egelstaff, in *Neutron Scattering* (National Technical Information Service, Springfield, Va. 1976).
- ⁵J. L. Lebowitz, J. K. Percus, and J. Sykes, *Phys. Rev.* **188**, 487 (1969).
- ⁶T. Reed and K. Gubbins, *Applied Statistical Mechanics* (McGraw-Hill, New York, 1973).
- ⁷E. P. Gross and E. A. Jackson, *Phys. Fluids* **2**, 432 (1959); P. F. Bhatnagar, E. P. Gross, and M. Krook, *Phys. Rev.* **94**, 511 (1954).
- ⁸See, for example, J. Hopps, *Phys. Rev. A* **13**, 1226 (1976).
- ⁹R. C. Desai, *J. Chem. Phys.* **44**, 77 (1966); R. C. Desai and M. Nelkin, *Nucl. Sci. Eng.* **24**, 142 (1966).
- ¹⁰S. Yip and M. Nelkin, *Phys. Rev.* **135**, 1241 (1964).
- ¹¹S. Hess, *Physica* **61**, 80 (1972), Sec. 4.2.
- ¹²E. Smith, J. Cooper, and T. Dillon, *J. Quantum Spectrosc. Radiat. Transfer* **11**, 1547 (1971).
- ¹³J. A. McLennan, *Phys. Fluids* **9**, 1581 (1966).
- ¹⁴C. Cercignani, *Mathematical Methods in Kinetic Theory* (Plenum, New York, 1969).
- ¹⁵J. R. Dorfman and H. van Beijeren, in *Statistical Mechanics*, Part B, edited by B. J. Berne (Plenum, New York, 1977).
- ¹⁶S. Yip (private communication).
- ¹⁷A. Z. Akcasu and J. Duderstadt, *Phys. Rev.* **188**, 479 (1969); G. Mazenko, *Phys. Rev. A* **5**, 2545 (1972); **9**, 360 (1974).
- ¹⁸The hard-sphere limit of this equation ($\beta V_0 \rightarrow \infty$) has been discussed in Ref. 3.
- ¹⁹A. R. Altenberger, *Physica A* **80**, 46 (1975).